THE ROLE OF FGF GROWTH FACTORS IN THE DEVELOPMENT OF CHEMOTHERAPY DRUG RESISTANCE IN OVARIAN CANCER CELLS

By

Albatul Awadh Alharbi

A thesis submitted in partial fulfillment

of the requirements for the degree of

Master of Science (M.Sc.) in Biology

School of Graduate Studies

Laurentian University

Sudbury, Ontario

THESIS DEFENCE COMMITTEE/COMITÉ DE SOUTENANCE DE THÈSE
Laurentian Université/Université Laurentienne
Faculty of Graduate Studies/Faculté des études supérieures

Title of Thesis
Titre de la thèse THE ROLE OF FGF GROWTH FACTORS IN THE DEVELOPMENT OF CHEMOTHERAPY DRUG RESISTANCE IN OVARIAN CANCER CELLS

Name of Candidate
Nom du candidat Alharbi, Albatul

Degree
Diplôme Master of Science

Department/Program
Département/Programme Biology

Date of Defence August 31, 2015
Date de la soutenance

APPROVED/APPROUVÉ

Thesis Examiners/Examinateurs de thèse:

Dr. Carita Lannér
(Supervisor/Directeur(trice) de thèse)

(Co-supervisor/Co-directeur(trice) de thèse)

Dr. Mazen Saleh
(Committee member/Membre du comité)

Dr. Amadeo Parissenti
(Committee member/Membre du comité)

Dr. Madhuri Koti
(External Examiner/Examinateur externe)

Approved for the Faculty of Graduate Studies
Approuvé pour la Faculté des études supérieures
Dr. David Lesbarrères
Monsieur David Lesbarrères
Acting Dean, Faculty of Graduate Studies
Doyen intérimaire, Faculté des études supérieures

ACCESSIBILITY CLAUSE AND PERMISSION TO USE

Abstract

Ovarian cancer is the most gynecological cancer, it has a 5-year mortality rate greater than 70%. When ovarian cancer patients undergo chemotherapy their gene expression changes. This project is studying a particular group of genes called Fibroblast Growth Factors (FGFs), which have been found to be very important in cancer. The hypothesis predicted that significant changes in the expression of FGF proteins are associated with the development of drug resistance in ovarian cancer. Previous work developed three resistant cell lines from the A2780 ovarian cancer cell line (A2780CBN, A2780DXL, A2780CBNDXL), In the previous studies, microarray analysis was performed to find changes in gene expression in the three cell lines. We have been able to confirm some of the changes that indicated a possible role for FGF gene expression changes in drug resistance. However, we could only confirm a change in protein expression for one of the FGF factors, FGF23, which was altered in A2780CBN and A2780CBNDXL resistant cell lines.

Acknowledgment

First of all, my deepest acknowledgement goes to my thesis supervisor, Dr. Carita Lanner for her understanding, patience and mentoring me step by step through the whole research process and for pushing me further than I thought I could go. To my supervisory committee, Dr. Amadeo Parissenti and Dr. Mazen Saleh, I am extremely grateful for your assistance and suggestions throughout my project.

My mother, father, thanks for your support and unconditional love. Even though I am thousand of miles away, you were always there whenever I needed you. Thank you both for helping me survive all the stress and not letting me give up. I love you!

This thesis would have never been possible without my loving husband Abdulrahman.You were always around at times I thought that it is impossible to continue, you helped me to keep things in perspective; you are a wonderful man and I am truly blessed to share my life with you. I must give special thanks to you.

My lovely children Aseel and Basel, I owe you lots and lots of fun hours. I couldn’t imagine doing my master's degrees without you; you really gave me the reason to continue. Words would never say how grateful I am to both of you.

Table of contents

Appendices

List of Figures

List of Tables

Introduction

Ovarian Cancer

Cancer is a major cause of death in women throughout the world. In Canada, it is estimated that 76 000 deaths will be due to cancer in 2014 it is responsible for 30% of all deaths[2]. Ovarian cancer is the most lethal gynecological cancer and it is responsible for 5% of cancer deaths[3] . The reason for the increased mortality is because women who have ovarian cancer do not show any early symptoms and early diagnosis has not been successful. Symptoms that can be observed in women with ovarian cancer are usually not clear, for example unusual bloating, abdominal fullness, pressure, difficulty eating and back pain, and these symptoms are vague and obscure [4]. Because of this, more than 70% of women are diagnosed at late stages [5]. To describe the growth or spread of ovarian cancer, there are four stages: I through IV. Staging is very important because ovarian cancer has different stages and they are treated differently. Each stage is divided into three subtypes except stage four. Stage I refers to ovarian cancer that is located inside or associated with the ovaries only. Stage II refers to ovarian cancer that is located in one or both ovaries and has spread into the pelvis. Stage III ovarian cancer has grown outside the area of the pelvis into the abdominal cavity, also if cancer is found in lymph node it is considered to be stage III. Stage IV describes ovarian cancer that has spread (metastasized) to distance organs such as the liver and lungs. However if the cancer is found only on the surface of organs and not penetrating the organs themselves, the cancer is described as stage III.

Based on the staging criteria, it is not difficult to understand that the five years survival rate for women with stage III and stage IV disease is lower than 20% [6].

Ovarian cancer is classified into different types. Epithelial ovarian cancer is the most common type and accounts for approximately 90% of malignant ovarian tumours [7], and these tumours are derived from the surface of the ovarian epithelium. The other two ovarian tumour types that are not derived from the epithelum, are stromal and germ cell tumours. These tumors are not as common as epithelial-derived tumors. Epithelial ovarian cancer is classified based on histopathology which observes changes in the tissues caused by the cancer, immunohistochemistry which is the process of detecting specific antigens in tissues by staining with antibodies labeled with fluorescent material, and molecular analysis which is a method of classifying disease by analyzing DNA or RNA transcripts, into high grade-serous, low grade-serous, endometrioid, clear cell and mucinous carcinomas [8]. About 70% of deaths are seen in patients with high grade-serous ovarian carcinomas [9].

High grade serous (HGS) carcinoma is the most common type of ovarian carcinoma which accounts for 70% of all cases of ovarian cancer. Mutations in the p53 and BRCA 1, 2 genes are frequent in high grade serous carcinoma. High grade serous carcinomas are the most common in North America. Despite the high mortality rate, high grade serous ovarian cancer has an initial 80% response rate to chemotherapy drugs [8, 10]. Although HGS ovarian cancer has a high response rate to chemotherapy, the mortality rate is still high because the majority of women have recurrence of treatment-resistant tumours.

Low grade serous carcinoma is not as common and accounts for < 5% of the cases [8]. It is usually diagnosed at high stage. Genetic abnormalities common to low grade serous ovarian cancer are different from high grade serous carcinoma. Approximately between 20% to 40% of low grade serous carcinomas have a dysregulation in the KRAS

gene, however only 5% of low grade serous carcinoma have mutaions in the BRAF gene [11]. Initial treatment of low-grade serous carcinoma involves surgery and platinum-based chemotherapy. However, treatment for relapses is secondary cytoreduction, salvage chemotherapy or hormone therapy [11]

Mucinous carcinomas are much less common in ovarian cancer, only 3% of ovarian carcinomas are of the mucinous type. It is well known that mucinous carcinomas have a poor response rate to chemotherapy. Mutations in KRAS are the most common mutation found in mucinous carcinomas. HER2 amplification is also present in mucinous carcinomas [8] [12].

Endometrioid carcinomas are more common and account for approximately 10% of all cases of ovarian cancer. Most are found in stage I or II and need no additional treatment after surgery. Higher stages of endometrioid carcinomas are often treated with chemotherapy such as carboplatin, paclitaxel and combination chemotherapy of carboplatin with paclitaxel [13]. The most common genetic dysregulations in endometrioid carcinoma are somatic mutations in CTNNB1, KRAS, ARIDIA and PIK3CA. In addition, there are less common mutations, including genes like PTEN, PPP2R1A and TP53 [8, 14] . The response rates to treatment have been reported to be between 10-15%.

Clear cell carcinomas present at a similar percentage as endometrioid carcinomas which is 10% and they are more common in the Asian population [8, 10]. Clear cell carcinoma has a 15% response rate to chemotherapy treatment , demonstrating that this type of ovarian cancer does not respond well to chemotherapy. However, it has been reported that there are positive effects of combined radiation and chemotherapy[15]. The

molecular markers of clear cell carcinoma are mutations in ARID1A, PTEN, PIK3CA and HNF-1B [16].

Besides the type of ovarian cancer, treatment of ovarian tumours depends on the stage of cancer. Because most of the disease is diagnosed at a late stage, treatment typically involves removal of the bulk of the tumour as the main treatment for most ovarian cancers, followed by chemotherapy, which is a drug that is used to kill cancer cells by stopping them from growing and dividing. In the 1940's, alkylating agents were the earliest drugs that were used to treat ovarian cancer, including melphalan, ifosfamide and chlorambucil [17]. In the 1970's, platinum agents were found to show more effectiveness after alkylating agents [18].

There are two different methods used to deliver chemotherapy to ovarian cancer patients. The first option is to give the patient the drug by the intravenous (iv) route which is to deliver the chemotherapy into a vein. The other option, intraperitoneal delivery, is to have the chemotherapy delivered directly to the abdominal cavity by using a thin tube [19]. In the two different types of administration, the same chemotherapy regimens are used (cisplatin-carboplatin and paclitaxel), but the dosing schedule is different. Intraperitoneal delivery has a significant improvement in long-term progression-free survival (PFS) and overall survival (OS) compared with intravenous (IV) chemotherapy [20]. Evidence provided by M. Fung-Kee-Fung *et al.* suggested a significant survival benefit for cisplatin IP chemotherapy in patients with epithelial ovarian cancer stage III [21]. Another advantage of intraperitoneal delivery is that higher concentrations of drug could be used, in addition to demonstrating a longer half-life of drug compared with intravenous route. However, toxicity is more frequent with IP than

with IV and the most common symptoms of toxicity are abdominal pain, fatigue and metabolic toxicities [22].

Unfortunately, chemotherapy drugs are not only killing cancer cells, they also harm healthy cells (cytotoxicity), which causes side effects. These can occur with any type of treatment for ovarian cancer and include symptoms such as nausea and vomiting, loss of hair, diarrhea and allergic reactions.

Currently, standard chemotherapy for most types and stages of ovarian cancer consists of platinating agents and/or taxanes[23]. Many patients achieve complete clinical response following the treatment, but often, patients will have a recurrence and present with disease after treatment. In addition, they typically develop drug resistance and stop responding to the chemotherapy agents [24].

Platinating Agents – Mechanisms of Action

Platinating agents are drugs that used clinically to treat different types of cancer such as head and neck, ovarian, lung and testicular [25] . The chloride ions on the platinum drugs are usually replaced by water molecules once they enter the cell. Positively charged platinating agents will interact with nucleophilic DNA, forming adducts that change DNA structure. Platinating agents react with the N7-atom of guanine or adenine residue. Platinating agents form many type of adducts: monoadducts, intrastrand crosslinks and interstrand crosslinks. Monoadducts form when the platinating agent binds to only one nucleotide, usually adenosine or guanosine. When monoadducts bond again to another adenosine or guanosine, most of the monoadducts react further to form crosslinks [25]. Intrastrand crosslinks form when the platinating agent binds to two nucleotides on the

same strand of DNA. Most of the crosslinks are intrastrand. Interstrand crosslinks form when platinating agent binds to two nucleotides on opposite DNA strands. As a result, formation of DNA adduct can induce different cell death pathways.

Platinating agents can also have toxic effects that cause damage to patients' organs. Ototoxicity is present in a high number of patients who received high doses of platinating drug [26]. Cisplatin has been found to target cochlear hair cells resulting in damage to hearing. The mechanism of action might be the production of reactive oxygen species (ROS) that lead to cell death by apoptosis [26].

Reactive oxygen species (ROS) is also another mechanism of cisplatin, however the detailed mechanism is still unclear. Reactive oxygen species are produced by the mitochondria which cause cell death upon exposure to cisplatin. It has been reported that DNA integrity, bioenergetics functionality and mitochondrial redox status are important inducers of cellular response to cisplatin-induced mitochondrial damage. Moreover, it has been shown by Marullo *et al.* that reactive oxygen species are observed *in vivo* after exposure to cisplatin in several tissues[27].

Taxane Agents – Mechanisms of Action

Taxanes are cytotoxic drugs that are used as a first line treatment in ovarian cancer. Taxanes (paclitaxel) are isolated from the bark of the yew tree. Taxanes include paclitaxel and docetaxel. The principal mechanism of action of taxanes is the disruption of microtubule depolymerization. Microtubules play an important role in cell division and maintaining cell shape. Microtubules are composed of alpha and beta tubulin

heterodimers. Taxanes interfere with the depolymerisation of microtubule resulting in cell cycle arrest and apoptosis. When a comparison is made between the two most commonly used taxanes, docetaxel was found to have 1.9 fold higher affinity for the beta-tubulin binding site compared to paclitaxel [28].

Apoptotic pathway induction caused by disruption of microtubule structure via taxane drugs is an important mechanism of taxanes. Damage of microtubules by taxanes induces Bcl2 protein hyperphosphorylation that plays an important role in regulation of apoptosis. Hyperphosphorylation of Bcl2 induces apoptosis.

Taxanes can also induce Reactive oxygen species (ROS) at a high level which leads to apoptosis. Reactive oxygen species can cause significant damage to cells when they reach high concentrations. This damage includes DNA damage, protein and lipid oxidation, which leads to cell apoptosis [29].

Ovarian Cancer and Chemotherapy Resistance

One of the major problems associated with chemotherapy treatment is the development of drug resistance. Approximately 70% of the patients undergoing treatment for advanced stage tumours will develop recurrent disease [1]. To understand how to overcome drug resistance, it is important to understand the mechanisms that play a role in the development of chemotherapy drug resistance.

Mechanisms of resistance to Platinating Agents

The platinating agents most commonly used are cisplatin and carboplatin. These are drugs containing platinum which interact with a DNA, RNA and protein functions [25].

Platinating agents target DNA more, compared to other molecules, causing cell cycle arrest, apoptosis and signaling DNA damage response [30].

A major mechanism of resistance to platinating agents is reducing the amount of drug entering the cell [25]. Copper transporters are associated with platinating agent resistance. The copper transporter CTR1 regulates cisplatin uptake [31]. It has been reported that knockdown of CTR1 is associated with decreasing cisplatin uptake by 80% in both mouse embryonic fibroblasts and yeast [32, 33]. The other two copper transporters that are involved in resistance to cisplatin are ATP7A and ATP7B. Deactivation of their transporter activity is linked with decreasing copper efflux from cells. It has been reported that overexpression of ATP7A in the 2008 human ovarian cancer cell line induced resistance to cisplatin, carboplatin and oxaliplatin. Furthermore, high levels of copper efflux transporter ATP7A and ATP7B are linked with a poor response in patients with ovarian cancer receiving cisplatin or carboplatin-based chemotherapies[34].

DNA repair is also one of the most important mechanisms involved in platinum resistance. Nucleotide excision repair is one of the DNA repair pathways that happen when a DNA adduct is formed and alter the shape of the DNA helix. This damage is excised by the excision repair cross complementation group 1 (ERCC1) and xeroderma pigmentosum complementation group F (XPF) proteins. In the absence of ERCC1 and XPF, the DNA will not be repaired leading to cell death[35]. Another pathway that is involved in repairing adducts induced by platinating agents is the mismatch repair pathway. Mismatch repair occurs when the Mut protein recognizes unmatched DNA base pairs caused by platinating agents and induces apoptosis. Therefore, absence of MMR

mechanism leads to carboplatin resistance [35, 36]. The study by Fink, D. *et al.* showed an association between loss of the DNA mismatch repair proteins, which recognize the DNA damage caused by platinum agents and decreasing level of resistance to drugs [37].

Mechanisms of resistance to Taxanes

Taxanes such as docetaxel and paclitaxel stabilize microtubules by stopping depolymerisation, which is important for proper continuation of the cell cycle [38]. By binding strongly to the β-tubulin subunit of the microtubules, taxanes cause cell cycle arrest, which leads to cell death [39]. Resistance to taxanes can occur because of increased expression of p-glycoprotein efflux pumps, which is a common mechanism that is involved in resistance to taxanes. The P-glycoprotein, ABCB1, is a member of the ATP-binding cassette (ABC) transporter family that enables the efflux of many anticancer drugs including taxanes [40]. High-level expression of the ABCB1 gene results in decreasing the concentration of taxanes. A study done by Ehrlichova *et al*. [41] using human breast cancer cells showed via Reverse Transcription Polymerase Chain Reaction (rtPCR) that resistant cells expressed a high level of p-glycoprotein mRNA compare to the parental sensitive cell line. Another study by Hembruff, S.L. *et al*. indicates that there is a relationship between the expression of drug transporters in MCF-7 breast cancer cells and the resistance to docetaxel [42].

Another mechanism that is involved in resistance to taxanes and has the ability to deactivate the drug are cytochrome p450 enzymes. Cytochrome p450 is known to metabolize a wide range of anticancer drugs [43]. The CYP1B1gene is a member of the

P450 family of cytochromes that are present in many types of malignant tumors and in metastatic disease [44]. It has been reported by McFadyen *et al.* that transfection of CYP1B1 leads to increased resistance to docetaxel in V79 cell lines [43]. Another study that also was done by McFadyen *et al.* using the chinese hamster ovary, CHO, cell line which expresses cytochrome CYP1B1, exposed the cells to docetaxel. A high increase in resistance to docetaxel in the cell line expressing CYP1B1 was observed compared to the parental cell line (P= 0.03) [43].

Another mechanism of resistance to taxanes is alterations in β-tubulin, either by increased expression or by mutation in the gene [45]. Transfection of Chinese hamster ovary (CHO) cells were used to determine whether β-tubulin mutations found in cancer cells have the ability to induce resistance to taxanes in microtubules. The results showed that there were three mutations (A185T, A248V and R306C) which caused paclitaxel resistance. This mutations cause alterations in microtubules, induce sensitivity to microtubules-disruptive drug and cause deficiency in mitosis[46].

In general, lack of response to chemotherapy drugs is linked with changes in gene expression, and epigenetic changes that affect drug uptake, metabolism of the drug, or export of drugs from tumour cells [47]. Because of increased variability from one patient to another and the complexity of involvement of the circulatory system, it is difficult to understand the main mechanism of resistance for different chemotherapy agents in a clinical setting.

Model Systems to Study Drug Resistance

Several *in vitro* and *in vivo* cancer models have been developed from cancer cell lines to study the mechanisms of drug resistance that affect cancer treatment. There are limitations of using *in vitro* models such as lack of a diverse cell population as observed in patient tumours, but *in vitro* cell culture can provide useful information such as drug sensitivity, cell biology and in the identification of signalling pathways that are affected by drug exposure [48].

To understand how drug resistance plays a very important role in the development of chemotherapy resistance in ovarian cancer, researchers have developed resistant cell lines by selecting for cells that are able to grow in the presence of increasing chemotherapy drug concentrations [49]. In the clinical setting, ovarian cancer patients are often treated with carboplatin together with paclitaxel, although docetaxel is also used as an alternative to paclitaxel because of reduced toxicity but similar effectiveness [50]. To understand how this dual agent chemotherapy, used for treatment of advanced ovarian cancer, is also able to cause development of resistance in patients, our research group has developed several drug resistant ovarian cancer models based on the A2780 cell line [1]. Our group has developed cell lines resistant to single agents, such as carboplatin (A2780CBN) and docetaxel (A2780DXL), in addition to a dual agent resistant cell line, the A2780CBNDXL line. Resistant cell lines were established by propagating cells in media containing increasing concentrations of carboplatin alone, docetaxel alone or in the presence of both carboplatin and docetaxel. Armstrong *et al.*, demonstrated that cells exposed to combination chemotherapy showed distinct genetic alterations, compared to gene expression changes seen in the single agent resistant cell lines. Armstrong *et al.* used microarray analysis, which is a widely used genomic tool that allows for profiling of

mRNA expression of thousands of genes at once to identify changes in gene expression associated with drug resistance [51].

cDNA microarray analysis uses an array of thousands of microscopic spots of oligonucleotides of specific DNA sequences arranged on slides to which cDNA sequence of samples can hybridize [52]. To perform the microarray analysis, total RNA is extracted from cells, which is then used to generate cDNA using reverse transcription. cRNA is then generated which is labelled using a dye before applying the sample to the array. As a result, strength of the hybridization signal produced is because of the gene expression level of that particular gene [53].

Using this technique, thousands of gene expression changes were identified in the resistant cell lines when compared to the parental A2780 line. The microarray results showed significant changes in 3000 genes in the A2780CBN line, 4621 genes in the A2780DXL line and 4070 genes in the A2780CBNDXL line [1]. More analysis of the data and comparison between the three drug resistant cell lines showed the resistance seen in combination chemotherapy is not a combination of changes identified in the single agent resistant lines. Greater than 70 % of the total gene expression change was found to be unique to the A2780CBNDXL cell line [1]. The gene expression data obtained using the microarray experiments were further analyzed using Functional Interaction Network Analysis.

Functional Interaction Network analysis

Microarray generates thousands of different gene expression changes, but other analysis methods are needed to organize the observed changes to help identify pathways

affected by the genes. Therefore pathway analysis can be performed which identifies interactions between different genes or proteins to identify the pathways affected [54].

Previous work that was done in our lab performed microarray analysis to find changes in gene expression in the three cell lines that were developed from the A2780 ovarian cancer cell line. The microarray results were used to perform Functional Interaction Network (FIN) analysis, which was carried out by Dr. Irina Kalatskaya at the Ontario Institute for Cancer Research (OICR).

A FIN based analysis was performed on microarray data to identify genes that play a role in drug resistance. Genes with significantly different expression were included into the functional interaction network analysis. Linkers were identified between genes to connect them in one subnetwork using a minimum spanning tree algorithm, which automatically identifies gene clusters that define a signaling pathway.

Each of the three cell lines has several clusters that come up as significant. For example, there are significant clusters present in A2780CBN such as (cadherin, ECM, FGF and RhoGTPases) (Figure1) and in A2780DXL (TNF, GPCR, TGF and cell cycle) (Figure 2) whereas A2780CBNDXL which has the biggest number of clusters (collagen, P-glycoprotein, FGF and cadherin) (Figure 3).

Carboplatin (CBN) cluster

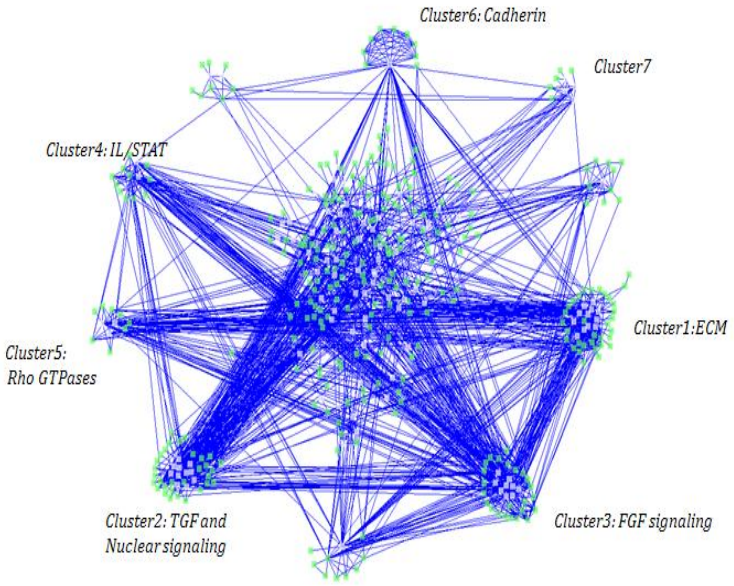

Figure1: Representation of A2780CBN cluster: there are several clusters that are significant in A2780CBN.

Docetaxel (DXL) cluster

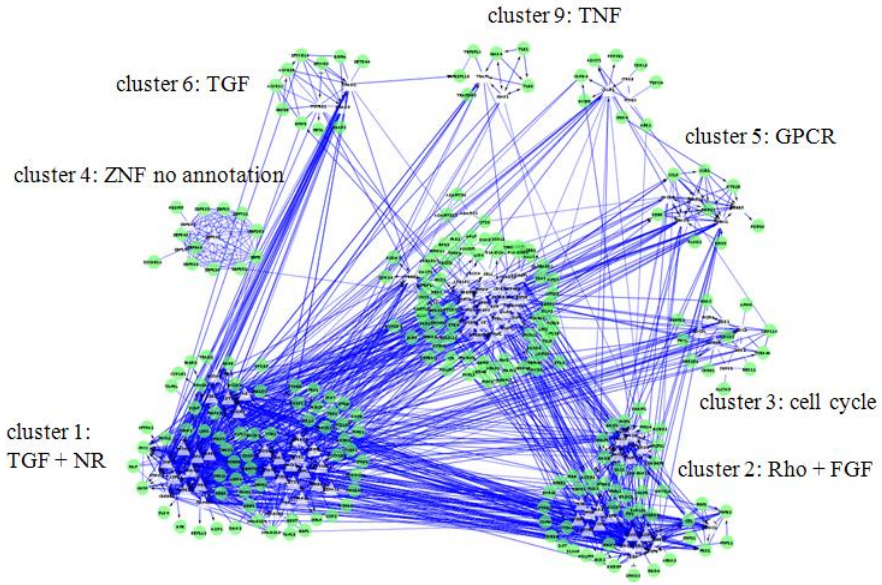

Figure2: Representation of A2780DXL cluster: there are several clusters that are significant in A2780DXL.

Dual (CBNDXL) cluster

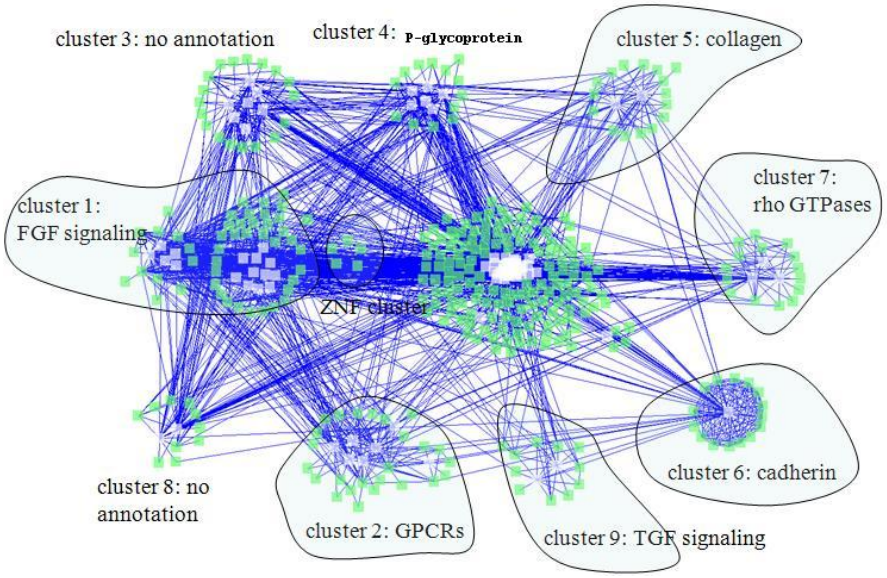

Figure 3: Representation of A2780CBNDXL cluster: there are several clusters that are significant in A2780CBNDXL.

To determine protein network validity we selected promising clusters from each cell line for validation which is the Fibroblast Growth Factor (FGF) cluster. There are several reasons for selecting the FGF clusters, which include the fact that the FGF cluster was present in the functional network analysis for each cell line and that the biggest cluster was found in the A2780CBNDXL. The microarray analysis had shown the greatest number of changes was in the A2780CBNDXL cell line, so the large FGF cluster in this cell line seemed to validate the microarray results. In addition, changes in the expression of FGF proteins are common in many types of cancers, some of which may play an important role in drug resistance. Moreover it is well-known that FGF proteins are altered in ovarian cancer.

Fibroblast Growth Factors

Normal role of FGF factors

Fibroblast growth factors (FGFs) play a fundamental role in developmental processes. During embryonic development FGFs are found to be important in many aspects such as regulating cell proliferation, migration and differentiation. In adult life, FGFs are crucial for tissue repair.

The human FGF family is a large family consisting of 22 members (FGF-1 to 14 and FGF-16 to 23). The FGF family is divided into six subfamilies depending on phylogenetic analysis and similarities in sequence: FGF1 and FGF2, the FGF3 family (FGF3, FGF7, FGF10, FGF22), the FGF4 family (FGF4, FGF5, FGF6), the FGF8 family (FGF8, FGF17, FGF18), the FGF9 family (FGF9, FGF16, FGF20) and the FGF19 family

(FGF19, FGF21, FGF23). An additional group, the FGF11 subfamily (FGF11, FGF12, FGF13, FGF14) is not considered to be a true member of the FGF family, despite sequence similarity to the FGF factors, because the FGF11 subfamily regulates voltage-gated sodium channels and does not bind to FGF receptors. To indicate this difference, the FGF11 subfamily are called fibroblast homologous factors (FHF) [55]. All the FGF growth factors, except FGF1, FGF2, and the FGF-9 subfamily, have signal peptides which allow the proteins to be released outside the cells. Cellular production of the FGF9, FGF16, and FGF20 subfamilies are through the endoplasmic reticulum (ER) – Golgi secretory pathway, whereas the FGF1 and FGF2 subfamily are produced in the cytoplasm [56]. The FGF proteins can be divided into groups as having paracrine effects which targets cells that are close to the cells producing the hormones and affects cells of a different type (FGF1, FGF2, FGF4, FGF8 and FGF9 subfamilies). FGF factors with endocrine effects are hormones that enter the blood circulation directly and travel to distant target organs (FGF19 subfamily) while intracrine FGF proteins act inside cells (FGF11-14). Paracrine and endocrine FGFs act through cell-surface FGF receptors (FGFRs) [57].

Fibroblast growth factors (FGFs) bind fibroblast growth factor receptors (FGFRs) which are tyrosine kinase receptors. There are 7 main FGFR isoforms (FGFR1b, FGFR1c, FGFR2b, FGFR2c, FGFR3b, FGFR3c and FGFR4). The b and c isoforms are alternatively spliced isoforms which are tissue specific. The b isoforms are expressed in epithelial tissues while the c isoforms are expressed in mesenchymal tissues. FGF receptors are composed of three important structures: extracellular immunoglobulin domains (D1-D3), a single transmembrane domain and a cytoplasmic tyrosine kinase

domain (Figure 1). There is also an acid box region, located between the D1 and D2 domains which plays an important role in receptor autoinhibition. The D3 domain is important for determining ligand specificity of the FGFR. Alternative splicing of the D3 domain can form the b and c isoforms of FGFR1, FGFR2 and FGFR3. (Figure 4) [55]

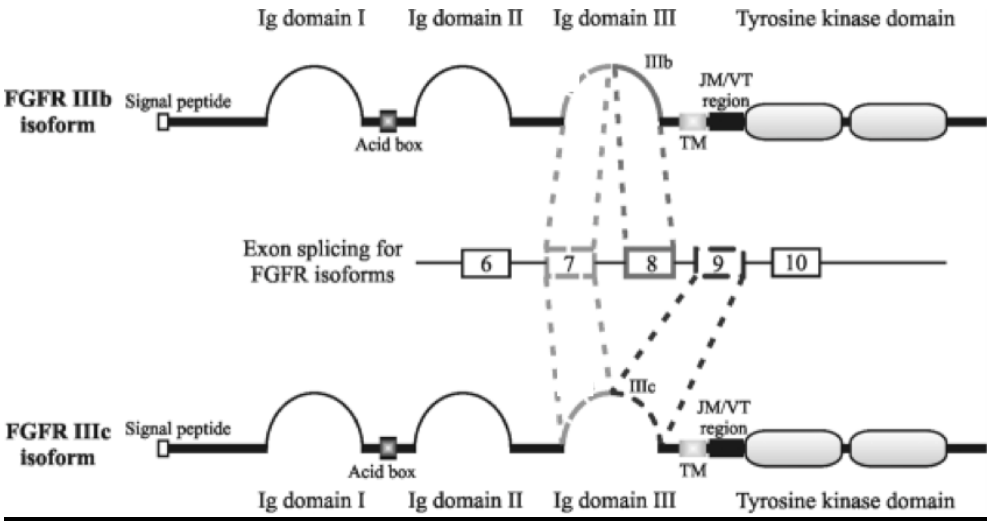

Figure 4: The two main structures isoforms of (FGFRs1-3), the alternative splicing of (b and c) are produced in the second half of D3 domain region [58].

FGF signaling pathways

When FGF: FGFR bind to each other, it will cause dimerization of two FGFRs and the activation of the intracellular kinase domain. Activation of the kinase domain occurs through transphosphorylation of the paired kinase domains. Other important activation changes are phosphorylation of the c-terminal ends of the receptors, phosphorylation of the juxtamembrane region and kinase insert. There are two main FGF signaling pathways which are the phospholipase C gamma (PLC-γ) (also called FRS1) and the FGFR substrate 2 (FRS2) pathway.

PLC-γ pathway activation requires tyrosine 766 (y766) in the FGFR, located at the C-terminal end of FGFR, to be autophosphorylated. PLC-γ can bind to the phosphorylated tyrosine through its SH2 domains. This activation leads to hydrolysis of phosphatidyl-4,5-bisphosphate (PIP_2), producing inositol triphosphate (IP_3) and diacylglycerol (DAG) which leads to activation of protein kinase C (PKC). In the second important signaling pathway, the docking protein FRS2 binds to the juxtamembrane region of FGFR. Activation of a FGFR leads to phosphorylation of FRS2 which allows the adaptor proteins Grb2 and the protein tyrosine phosphatase, Shp2, to bind FRS2. The recruitment of the Grb2 and Shp2 proteins leads to formation of complexes with more Grb2 molecules and the son of sevenless (SOS) which eventually activate RAS, RAF and MEK resulting in activation of the mitogen-activated protein kinase (MAPK) pathway and the phosphatidylinositol 3-kinase –AKt (PI3K-Akt) signaling pathway.

FGF ligand and FGFR interactions

Interactions between FGF ligands and heparin or heparan sulfate (HS) proteoglycan (HSPG) in the extracellular matrix is essential for stabilizing FGF proteins and limiting their diffusion [59]. The interaction with heparin/heparin sulfate is also important for stabilizing the binding of the FGF ligands with their receptors.

Each FGF can bind to several different FGFR subtypes. FGF1 has the ability to bind all the FGFR subtypes (FGFR1, 2, 3, 4) while the other FGF factors bind to some of the receptor subtypes but not all [60]. For example, FGF3 and FGF7 bind to FGFR1, FGFR2 and FGFR3 but not FGFR4 [61].

In addition, each FGF receptor subtype can exist as two isoforms, the b and c isoforms. These isoforms are produced via alternative splicing of the transcripts. The isoforms are tissue specific in that the b isoforms are expressed in epithelial tissues while the c isoforms are expressed in mesenchymal tissues (Table 1). Only FGF1 can bind to both b and c isoforms of any receptor. The other FGF factors typically bind to either an epithelial isoform or the mesenchymal isoform of each receptor there are some exceptions to this, for example, the FGF4 ligand family can bind to both the b and c isoforms of FGFR1.

	FGFR1		FGFR2		FGFR3		FGFR4
	FGFR1b	FGFR1c	FGFR2b	FGFR2c	FGFR3b	FGFR3c	
FGF1	binds	binds	binds	binds	binds	binds	binds
FGF2	binds	binds		binds		binds	binds
FGF3	binds		binds				
FGF7			binds		binds		
FGF10	binds		binds				
FGF22			binds				
FGF4	binds	binds		binds		binds	binds
FGF5	binds	binds		binds			
FGF6	binds	binds		binds			binds
FGF8	binds	binds		binds		binds	binds
FGF17		binds		binds			
FGF18				binds		binds	binds
FGF9	binds			binds	binds	binds	binds
FGF16							binds
FGF20		binds					
FGF19				binds			binds
FGF21			binds	binds			
FGF23		binds				binds	binds

Table 1: The interaction between FGF ligands and FGFR1-3. The designations of b and c represent the alternative splicing of FGFR. The b isoform is expressed in epithelial tissue and the c isoform is expressed in mesenchymal tissue)

The role of FGF in cancer

Deregulation of FGFR signaling is associated with many human cancers. In cancer, FGFR have been found to become over activated by several mechanisms, including gene amplification, chromosomal translocation and mutations. FGFR alterations are detected in a variety of human cancers, such as breast, bladder, prostate, ovarian, endometrial and lung cancers. For example, the mutation Gly388Arg in FGFR4 has been found to be associated with breast and colorectal cancer [62]. The same mutation, Gly388Arg, is also associated with progression of human prostate cancer [63]. Another interesting example is that SNPs (single-nucleotide polymorphisms) within intron 2 in FGFR2 have been found to be associated with breast cancer [64]. In FGFR3 there were three somatic mutations in (G380/382R; K650/652M and K650/652T) that are associated with bladder cancer [65].

In ovarian cancer, mutations (SNPs) in the FGF2 gene may alter angiogenic potential which leads to the growth of serous ovarian cancer [66].

Besides FGF2, other forms of FGF have been found to be associated with ovarian cancer. For example, around 40% of ovarian endometrioid adenocarcinomas have constitutive activation of Wnt signaling associated with an oncogenic mutation in the beta-catenin protein and increased downstream FGF9 expression [67]. FGF9 was found to be both mitogenic and to stimulate cell invasion through matrigel in epithelial cell types. Amplification of chromosomal region 5q31-5q35.3, which is the most significant copy number abnormality associated with serous ovarian cancer, leads to over expression of FGF18 [68]. The overexpression of FGF18 caused migration, invasion, and

tumorigenicity of ovarian cancer cells. FGF16 is also another example that stimulates the proliferation of human ovarian adenocarcinoma cells (SKOV-3- OAW-42) [69] Concerning, FGF23, alteration of serum or plasma FGF23 are involved in ovarian cancer. It has been shown that serum or plasma FGF23 concentrations are higher in women with advanced-stage epithelial ovarian cancer [70].

FGF factors can also play a role in chemotherapeutic drug resistance or sensitivity. FGF2 has been found to increase the sensitivity of A2780 and MCF-7 cells to cisplatin [71], FGFR4 was also found to be a regulator of drug resistance in colon cancer[72].

Hypothesis and objectives

Fibroblast growth factors (FGFs) are important because they play a role in many types of cancer including in ovarian cancer. We have generated three drug resistant cell lines from A2780 parental cell line which are resistant to carboplatin (A2780CBN), docetaxel (A2780DXL), or a combination of carboplatin and docetaxel (A2780CBNDXL), and by using the resistant cell lines we can see if significant changes in expression of FGF proteins are contributing to the development of drug resistance in ovarian cancer.

The hypothesis of this study is to see if significant changes in expression of FGF proteins contribute to the development of drug resistance in ovarian cancer.

The objectives of this study are to validate changes in FGF/FGFR gene expression in cell lines by using QPCR technique to confirm changes in expression detected by microarray

analysis and to validate changes in FGF protein expression in the cell lines by Western blotting. In addition, I wish to knock down the expression of interesting FGF genes in in the A2780 cell line by using the siRNA technique and evaluate the effect of changes in expression on drug resistance by clonogenic assay.

Materials and Methods

Cell culture:

The human ovarian carcinoma cell line A2780 was purchased from the European Collection of Cell Cultures (ECACC, Salisbury, UK) and maintained in chemotherapy drug-free RPMI-1640 medium with 2 mM glutamine (HyClone, South Logan, Utah, USA). The medium also contained 10% FBS (HyClone, South Logan, Utah, USA), and 1% penicillin (10 000 I.U./mL)/ streptomycin (10 000µg/mL) solution (HyClone, South Logan, Utah, USA). A2780 cell lines resistant to docetaxel (A2780DXL), carboplatin (A2780CBN) and to both docetaxel and carboplatin (A2780CBNDXL) were generated by Armstrong *et al*. [1]. The A2780CBN and A2780DXl cell lines were maintained by adding $2.22x10^{-5}$M carboplatin and $4.05x10^{-7}$M docetaxel respectively, A2780CBNDXL cells were maintained by adding $6.07x10^{-6}$ M carboplatin and $6.07x10^{-9}$ M docetaxel. Cells were cultured in T75 flasks in a humidified incubator at 37^{o}C with 5% CO_2 and were checked microscopically daily to ensure they are healthy and growing as expected.

RNA extraction and analysis

RNA was purified using miRNeasy Mini Kit from Qiagen Laboratories (Mississauga, ON, Canada). The drug resistant A2780 cells were released from the flasks with trypsin and then counted using a ViCell counter (Beckman Coulter Inc., Mississauga ON, Canada). To count cells, the culture medium was collected and added to a 15 mL conical. The tissue culture dish was washed with PBS, which was also collected and added to the 15 mL conical tube and spun at 500 × g for 5 min to harvest the cells. A volume of 700µl

of QIAzol lysis solution was added to the plate and using a cell scraper, cells were gently scraped off the bottom of the flask into the lysis solution. Homogenization was done using a 20-gauge needle-fitted syringe for 1 minute, or until no clumps were visible. The tubes containing the homogenized samples were placed at room temperature (25° C) for 5 minutes, 140 µl of chloroform was added to the homogenate and vortexed for 15 seconds. This was important to induce phase separation. The tube was placed on the benchtop at room temperature for 2-3 minutes. At this time the separation of the solutions became visible. The sample was centrifuged at 12000 x g at 4° C for 15 minutes, and after centrifugation, the sample separated into three distinct phases; one upper colourless, aqueous phase containing the RNA; a white interphase containing the DNA; and a lower red organic phase containing proteins. The upper aqueous phase was transferred to a new collection tube, 525 µL of anhydrous ethanol was added to precipitate the RNA, and mixed by pipetting up and down. Following precipitation, 700 µl of the sample was pipetted onto a RNeasy spin column that was placed in a 2 ml collection tube and centrifuged at 8000 x g for 15 seconds at room temperature. During centrifugation the RNA binds to the column membrane. The membrane was washed with 700 µl of the washing Buffer RWT, supplied in the miRNeasy mini kit, and centrifuged at 8000 x g for 15 seconds. The flow-through was discarded, and 500 µl of another washing buffer, Buffer RPE, also supplied in the miRNeasy mini kit, was added and centrifuged at 8000 x g for 15 seconds. The flow-through was discarded. Another 500 µl of Buffer RPE was added, and centrifuged at 8000 x g for 2 minutes. RNA was eluted by adding 50 µL of RNase free water to the spin column twice, and 1 µL of RNAase OUT (Invitrogen,

Carlsbad, CA, USA) was added to the RNA samples to prevent RNA degradation. The quantity of RNA in the above preparations was measured
using the NanoDrop ND-1000 spectrophotometer (Thermo Fisher Scientific Inc., Wilmington, DE, USA). RNA samples were stored at -80^{o}C.

QPCR analysis

cDNA preparation:

Gene expression can be quantified by measuring the expression of transcribed mRNA. Before mRNA can be quantified by (qPCR), the mRNA needs to be reverse transcribed into cDNA. Before, reverse transcription, DNAse treatment (Invitrogen, Carlsbad, CA, USA) of RNA was performed using 2µg RNA (use 1µg for cDNA preparation and keep 1µg in -80 ^{o}C), 2µl of 10X DNAse buffer, 2µl of DNAse AMP grade and PCR grade H_20 in a final volume of 20µl. The mixture was incubated for 15 min at room temperature, then 2µl of 25 mM EDTA was added to stop DNAse activity, the mixture was heated for 10 min at 65°C and directly used in cDNA production or stored at -80 °C. For the reverse transcription reaction, Superscript Reaction Kit (Invitrogen, Carlsbad, CA, USA) was used. A master mix was prepared from the kit reagents as shown in (Table 2).

Component	Volume of 1X Master Mix
5X buffer (first strand)	16µl
DTT (0.1M)	8µl
dNTP'S (10mM)	16µl
Oligo dt (20ng/ µl)	20µl
Random primers	4µl
RNAse OUT	4µl
Total	68µl

Table 2: cDNA Master Mix from the kit reagents

The reaction mix was incubated for 10 min at 37°C, 2µl of Moloney Murine Leukemia Virus Reverse Transcriptase (MMLV-RT) (Invitrogen, Carlsbad, CA, USA) was added, then incubated for 2 hours at 37°C, followed by heating for 5 min at 95°C to inactivate the MMLV-RT enzyme. Samples were stored at -20°C.

Real-Time PCR (Q-PCR) Reaction:

Real –time quantitative polymerase chain reactions (RT-QPCR) were performed on a Chromo4™ System machine (BioRad Laboratories, Inc., Mississauga, ON, Canada). Standard curves were prepared by diluting template cDNA four times (0.25x), and preparing further serial dilutions by diluting each step two times until a series is generated (0.25x, 0.125x, 0.0625x, 0.03125x, 0.015625x, 0.0078125x, 0.00390625x). Standard curves were generated for a housekeeping gene (28s rRNA) and for each gene being tested. Water was also included in the curves to check for random oligonucleotide contamination.

Samples were usually diluted 16x (0.0625x) to place their expression in the middle of the standard curve. Sometimes samples had to be used at a higher dilution, especially when the RNA concentration was low or if gene expression was naturally low.

	Forward	Reverse
	5' 3'	5' 3'
FGF1	ACGGCTCACAGACACCAAAT	TCTGGCCATAGTGAGTCCGA
FGF2	ACCCATCCCCTGGATATGCT	TGGCAGACGAATGCCTTATGT
FGF18	TATGCCCAGCTCCTAGTGGA	CATCAGGGCCGTGTAGTTGT
FGF20	AGAGGTGTGGACAGTGGTCT	GTGCCACAAAATACCTGCGG
FGF23	CAGACGCTGGAAAACGGGTA	CGTGGTATGGGGGTGTTGAA
FGFR1b	GCATTCGGGGATTAATAGCTC	CCACAGGTCTGGTGACAGTG
FGFR1c	ACCACCGACAAAGAGATGGA	GGACTCTCCCATCACTCTGC
FGFR2b	GATAAATAGTTCCAATGCAGAAGTGCT	TGCCCTATATAATTGGAGACCTTACA
FGFR2c	AGATTGAGGTTCTCTATATTCGGAATG	TTCTCTTCCAGGCGCTGG
FGFR3	CTGTCTGGGTCAAGGATGGC	AGCTTCTTGTCCATCCGCTC

Table 3: Primers used to amplify FGF target genes

NCBI Primer-Blast were used to design primers for the FGF1, FGF2, FGF18, FGF20, FGF23, FGFR1c, FGFR3 genes. Consensus coding sequences were found using the Ensembl database. Alignments between protein coding transcripts were done in the ClustalW program, Consensus coding sequences common to all transcripts were used to design primers (Table 3).

Primers for FGFR1b, FGFR2b and FGFR2c genes were designed by Coutu *et al.* [73]

Primers were purchased from (IDT Technologies, Coralville, Iowa, USA)

Western blot analysis

Cell lysates were prepared from three biological replicate cultures using mammalian protein extraction reagent, M-PER (Thermo Scientific, Rockford, IL, USA) lysis buffer containing HALT protease inhibitor (Thermo Scientific, Rockford, IL, USA), sodium fluoride (50 mM), sodium orthovanadate (0.2 mM),. Cells were collected using 0.25% trypsin-EDTA. Cell pellets were washed 3 times in PBS before being lysed with lysis buffer. Protein concentration in the lysates was determined using the Pierce BCA Protein Assay Kit (Pierce, Rockford, IL, USA). Cell lysate (20 µg protein per lane) was separated by 10% Polyacrylamide gel containing (SDS-PAGE). Proteins were transferred to BioTrace PVDF membrane (Life Sciences, Pensacola, FL, USA). Membranes were blocked with 5% milk solution in 1× TNE (obtained from a 20× TNE stock made using 100 mL of 1 M Tris-HCl (pH 7.5), 50 mL of 0.5 M EDTA (pH 8.0), 58.44 g of NaCl, H_2O to 500 mL) containing 0.1% Tween-20 (FisherBiotech, Thermo Fisher Scientific Inc., Waltham, MA, USA) for 1 hour. Primary antibody was diluted in milk and incubated with the membrane on a rocker over night at 4 ° C. After washing the

membrane for 3× 20 min in 1× TNE, the membrane was incubated with secondary antibody (Santa Cruz Biotechnology, Dallas, Texas, USA) diluted in 5% milk for 1 hour at room temperature, membranes then were washed for 6× 5 min in 1× TNE, the blots were incubated in enhanced chemiluminescence (ECL) reagents (GE health care, Mississauga, Ontario, Canada) and exposed to X-ray film (Thermo scientific, Mississauga, Ontario, Canada). Primary antibodies were from the following suppliers: FGF18 (cat. No ab86571, Abcam, San Francisco, California, USA), FGF20 (cat. No. AF2547, R&D Systems, Minneapolis, Minnesota, USA), FGF23 (cat. No. AF2604, R&D System, Minneapolis, Minnesota, USA). Secondary antibody suppliers were as follows: Goat anti-rabbit (Cat. No.ab97200, Abcam, San Francisco, California, USA), rabbit anti-goat (Cat. No.401515, CALBIOCHEM, San Diego, California, USA).

Small interfering siRNA gene knockdown experiments

In this study, siRNA against FGF23 was used to knock down expression of the FGF23 gene. Lipofectamine was used in this study to transfect siRNA into the cells. Lipofectamine® 2000 Reagent from Invitrogen™ (Waltham, Massachusetts, USA) was used to transfect siRNA into the A2780 cells. In short, cells were grown to about 30-50 % confluence. After counting, $300x10^3$ cells were plated per well (3 x 6-well plate) in 1.5ml RPMI+10% FBS without antibiotic, cells were incubated at 37^0C for 24hr. In a 24-well plate, siRNA and Lipofectamine® were diluted in serum-free Opti-MEM (Life technologies, Carlsbad, California, USA) before being combined and added to the cells. Lastly cells were incubated at 37ºC, 5% CO_2, for 24hr. Following transfection with

siRNA, total RNA was prepared from the transfected cells, using the Qiagen RNAeasy kit, and successful knockdown of gene expression was confirmed using RT-QPCR. Transfections with scrambled siRNA and GAPDH siRNA were used as negative and positive controls, respectively. The FGF23 siRNA and GAPDH siRNA were provided from Ambion® by Life Technologies.

Results

QPCR confirmation of expression in FGF factors

FGF1, FGF2, FGF18, FGF20, FGF23, FGFR1, FGFR2 and FGFR3 were selected based on the concurrence between the microarray data and the FIN analysis data that were compared to generate the group of FGF factors. These FGF factors were selected to confirm the level of change in the expression of the mRNA (Table 4). FGF1, FGF2, FGF18 and FGF23 are known to be involved in ovarian cancer [68, 70, 74]. Furthermore, FGF18 is involved in the cluster analysis in the A2780CBN and A2780CBNDXL cell lines. In the A2780CBN cell line, the expression of FGF18 was down regulated (-3.52) fold based on the microarray analysis, but was up regulated in the A2780CBNDXL cell line (7.27 fold) compared to the A2780 parental cell line based on the microarray analysis result (Table 4). FGF20 is not involved in the cluster analysis but in the microarray analysis, it has the biggest change in A2780CBNDXL cell line where it was down regulated (-131.53 fold) compared to the A2780 parental cell line. Expression of FGF20 has been found to be associated with the activation of the Wnt/β-catenin pathway [75]. Concerning the FGF receptors, both FGFR1 and FGFR2 have been reported in several studies to be involved in resistance to chemotherapy [76]. FGFR1 is also involved in the cluster analysis in two cell lines which are A2780CBN and A2780CBNDXL. FGFR3 is also involved in the cluster analysis in A2780DXL cell line.

	A2780CBN	A2780DXL	A2780CBNDXL
FGF1			
FGF2			-2.26
FGF3			
FGF4			
FGF5		-2.48	
FGF6			
FGF7			
FGF8			
FGF9		7.65	
FGF10		-2.58	
FGF11		-2.27	
FGF12			
FGF13	2.72		
FGF14	3.96	-4.77	-3.34
FGF15			
FGF16			
FGF17			
FGF18	-3.52, -3.48		7.26, 8.66
FGF19			
FGF20	-67.5	-16.26	-131.53
FGF21		-6.23	-3.67
FGF22			
FGF23			-13.4
FGFR1	2.03, 2.09, 2.26		-3.27
FGFR2			
FGFR3		-2.33	-2.11
FGFR4			

Table 4: Microarray fold changes in expression of FGF genes in the A2780CBN, A2780DXL, and A2780CBNDXL lines compared to A2780. Highlighted numbers indicate FGF genes which were also present in FIN result. Values in the table represent ratios of fluorescent values from the microarray between the parent and each cell lines and were calculated as described in Armstrong *et al.* [1]. Positive numbers mean upregulation of gene expression and negative numbers mean downregulation of gene expression

To investigate the level of expression of FGFs we compared the relative amounts of mRNA for each FGF factor in the A2780 resistant cells compared to A2780 parental cells using Qualitative Real-time Polymerase Chain Reaction (QPCR). Three biological samples were used for each FGF in the QPCR analysis. From the data obtained, for FGF1, there was no difference seen between the A2780 parental cells and the A2780 resistant cells (Figure 5). While the microarray analysis showed no difference in FGF1 expression between the A2780 parental cells and the A2780CBN resistant cells, the QPCR analysis was up regulated with a fold change of (3.1) but a P value for the QPCR analysis of 0.12 (Table 5). FGF1 from the microarray analysis also showed no change between the A2780 parental cell line and A2780DXL resistant cells. However, the QPCR analysis showed up regulation and has fold change of (2.3) (P= 0.48). In addition no expression seen in A2780CBNDXL cells in the microarray analysis, whereas the QPCR analysis showed (2.2) fold change and P value of (0.45). Based on the three QPCR comparisons between the A2780 parental cells and the drug resistant cells, there were no significant differences in the expression of FGF1.

FGF-1	Microarray	QPCR Fold change	P value
CBN	____	3.1	0.12
DXL	____	2.3	0.48
CBNDXL	____	2.2	0.45
FGF-2			
CBN	____	1.3	0.550
DXL	____	1.1	0.726
CBNDXL	-2.2	-2	0.288
FGF-18			
CBN	-3.4	-8.9	0.0037
DXL	____	-1.8	0.1293
CBNDXL	7.2, 8.6	1.0	0.9058
FGF-20			
CBN	-67.5	-68.6	1.97821E-05
DXL	-16.2	-6.9	0.0682
CBNDXL	-131.5	-135.7	0.0002
FGF-23			
CBN	____	-22.5	0.0065
DXL	____	-3.2	0.1299
CBNDXL	-13.4	-11.9	0.0075
FGFR1b			
CBN	____	2.5	0.220
DXL	____	-1.8	0.184
CBNDXL	____	-1.5	0.737
FGFR3			
CBN	-2.3	2.9	0.186
DXL	-2.1	2.2	0.859
CBNDXL	____	1.9	0.554

Table 5: Comparison of the microarray results with the QPCR results. The P values are calculated for each QPCR analysis comparing a resistant line to the parent line.

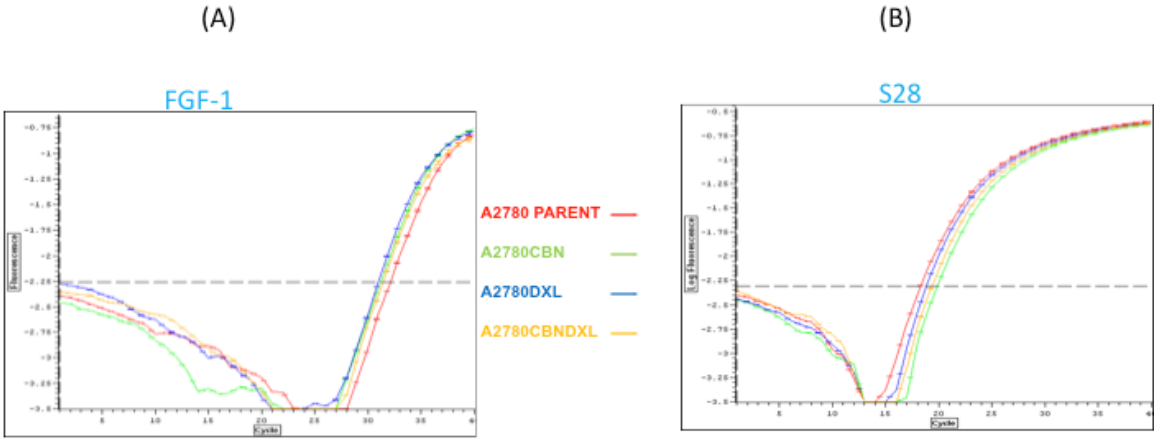

Figure 5: QPCR analysis of FGF1 expression in the A2780 parent and resistant cell lines. (A) Shows the QPCR analysis for FGF1. (B) QPCR for the S28 control in the A2780 parent and resistant cell lines.

A similar result was observed for FGF2; there was no difference shown between the A2780 parental cells and the three resistant cells (Figure 6, Table 5). From the microarray analysis, A2780CBN showed no expression change, whereas the QPCR analysis showed a low fold change of 1.3 and P=0.550 (Table 5). In addition, based on the microarray analysis, no change in expression was detected in A2780DXL, however the QPCR analysis indicated that there was a low expression in FGF2 with a fold change of 1.1 and a P value of 0.726. In A2780CBNDXL cells, both analyses indicated that the resistant cell lines were down regulated compared to the A2780 parental cell line with a fold change of about -2 and a P value of 0.288 (Table 5). Therefore, there were no significant changes in expression of FGF2 in any of the resistant A2780 cell lines.

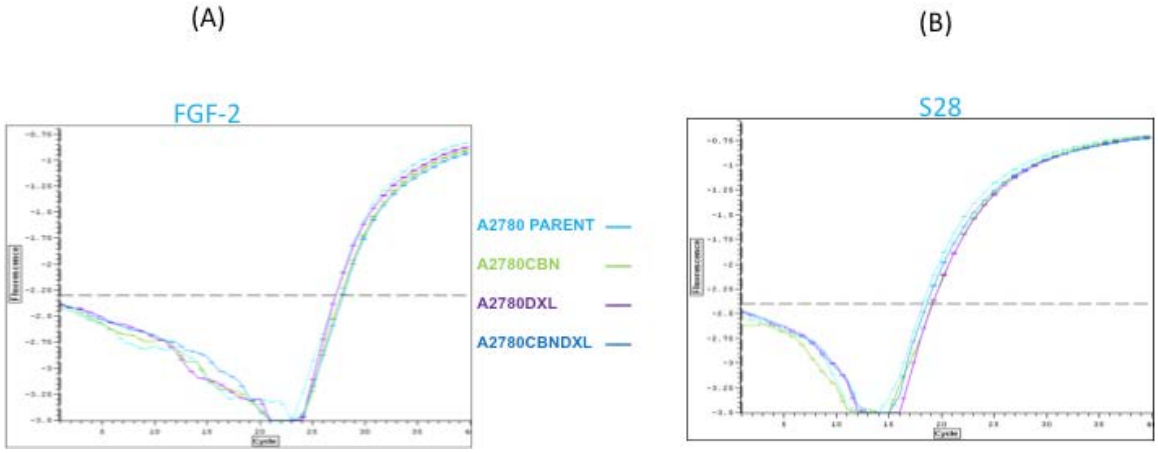

Figure 6: QPCR analysis of FGF2 expression in the A2780 parent and resistant cell lines. (A) The QPCR analysis for FGF2 (B) QPCR for he S28 control in the A2780 parent and resistant cell lines reaction.

Although the QPCR did not show any change in expression for FGF1 and FGF2, FGF18 showed an interesting change obtained from the QPCR analysis. A significant difference was seen between the A2780CBN resistant cells and the A2780 parental cells (Figure 7). The fold change was -8.9 with a P value of 0.0037 (Table 5). However, the microarray analysis showed a smaller fold change of -3.4. In addition, the microarray analysis showed no expression change in A2780DXL, whereas in the QPCR analysis there was a fold change of -1.8 but with a P value of 0.1293. The microarray analysis in the A2780CBNDXL cells showed an up regulation of 7.2 fold compared to A2780 parental cells. However, this number was not observed in the QPCR analysis, where only a 1.0 fold change compared to the parent with a P value of 0.9058. In summary, a significant change in FGF18 expression was observed in the A2780CBN cell line, based on QPCR analysis, but not in the A2780DXL or A2780CBNDXL cell lines.

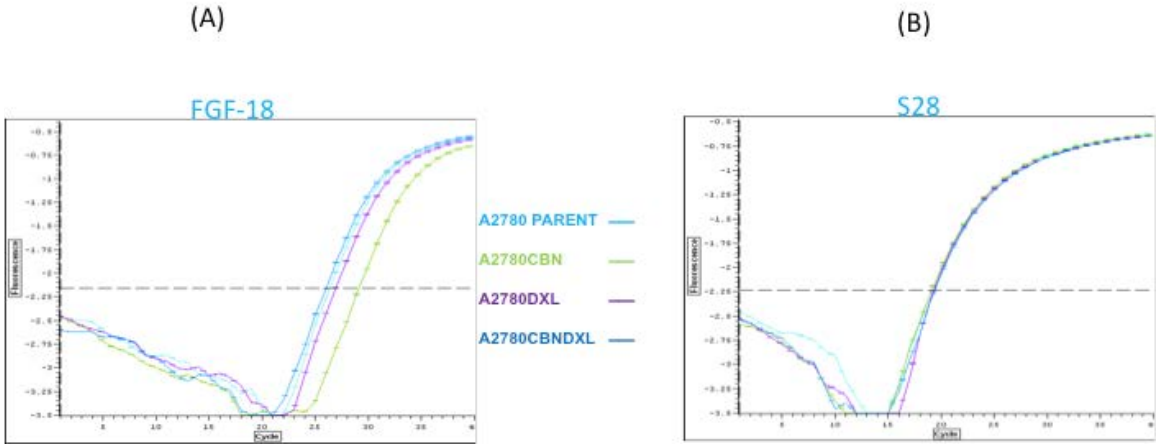

Figure 7: QPCR analysis of FGF18 expression in the A2780 parent and resistant cell lines. (A) QPCR analysis for FGF18 (B) QPCR for the S28 control in the A2780 parent and resistant cell lines reaction.

The data for FGF20 showed the most interesting change based on the QPCR analysis (Figure 8). There was a significant down regulation in A2780CBNDXL cells compared to A2780 parental cells in both the microarray and QPCR analysis, which have a fold change of -131.15 and -135.7 respectively with P= 0.0002 for the QPCR result (Table 5). A similar result was also observed in the A2780CBN cells which showed a significant difference compared to parental cells in both the microarray and QPCR analysis with a fold change of -67.5 and -68.6 respectively with P= 0.0000197 for the QPCR result (Table 5). However, although there was a difference in expression between the A2780DXL cells and the A2780 parental cells, it was not significant. The microarray result showed a -16.2 fold change, whereas the QPCR analysis showed -6.9 fold change with P= 0.0682 (Table 5). Based on these results, there is a significant difference in FGF20 expression in both the A2780CBN and A2780CBNDXL cell lines but not in the A2780DXL cell line.

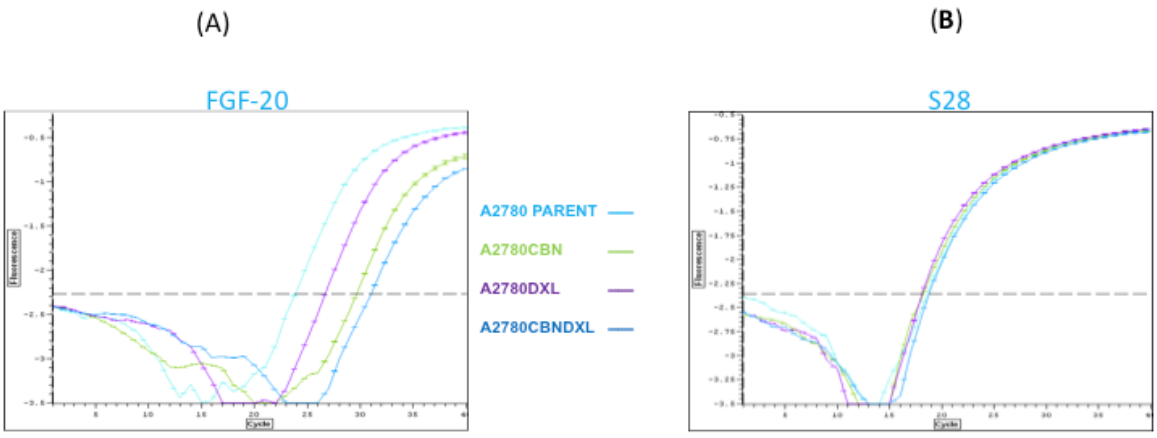

Figure 8: QPCR analysis of FGF20 expression in the A2780 parent and resistant cell lines. (A) QPCR analysis for FGF18 (B) QPCR for the S28 control in the A2780 parent and resistant cell lines reaction.

FGF23 also demonstrated a significant difference in expression in A2780CBN and A2780CBNDXL cells compared to A2780 parental cells (Figure 9). The microarray results showed no amplification in A2780CBN whereas in the QPCR analysis there was a significant change of -22.5 fold with a P=0.0065 (Table 5). In addition, A2780DXL cells showed no expression in the microarray analysis but the QPCR analysis showed a low fold change of -3 with P=0.1299 (Table 5). In A2780CBNDXL cells, both the QPCR and the microarry indicated that the resistant cells were down regulated compared to A2780 parental cell line with a fold change of -13.4 and -11.9 respectively and a P value of 0.0075 (Table 5). Therefore, both the A270CBN and A2780CBNDXL cell lines demonstrated a significant change in the expression of FGF23.

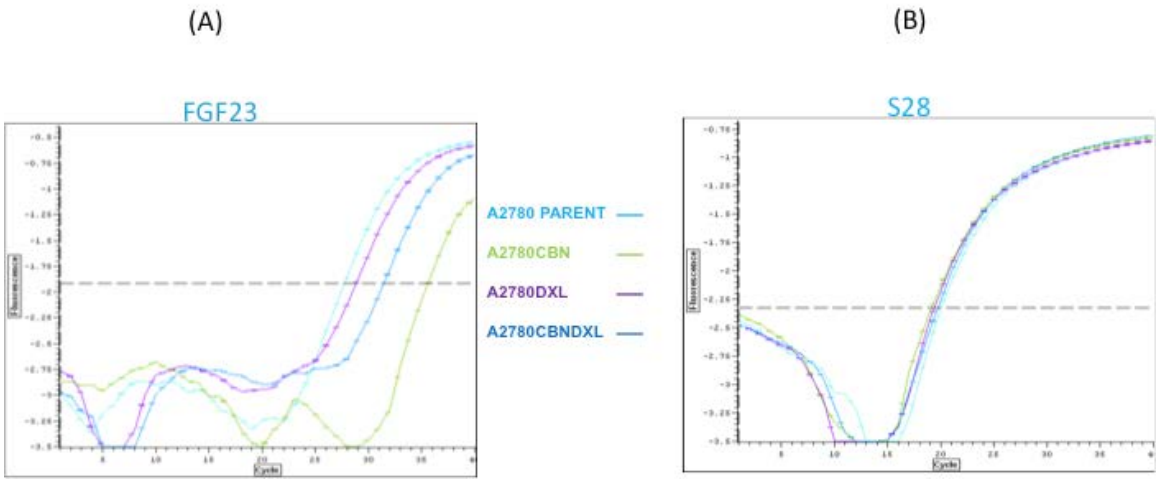

Figure 9: QPCR analysis of FGF23 expression in the A2780 parent and resistant cell lines. (A) QPCR analysis for FGF23 (B) QPCR for the S28 control in the A2780 parent and resistant cell lines.

The QPCR results for FGFR1b indicated that there was no difference between the A2780 parental cells and the three resistant cells (Figure 10, Table 5). The microarray analysis did not show any expression change in all three resistant cell lines, whereas the QPCR analysis illustrated that there was a low fold change of 2.5, -1.8 and -1.5 in A2780CBN, A2780DXL and A2780CBNDXL respectively, with P= 0.22, 0.184 and 0,737 (Table 5).

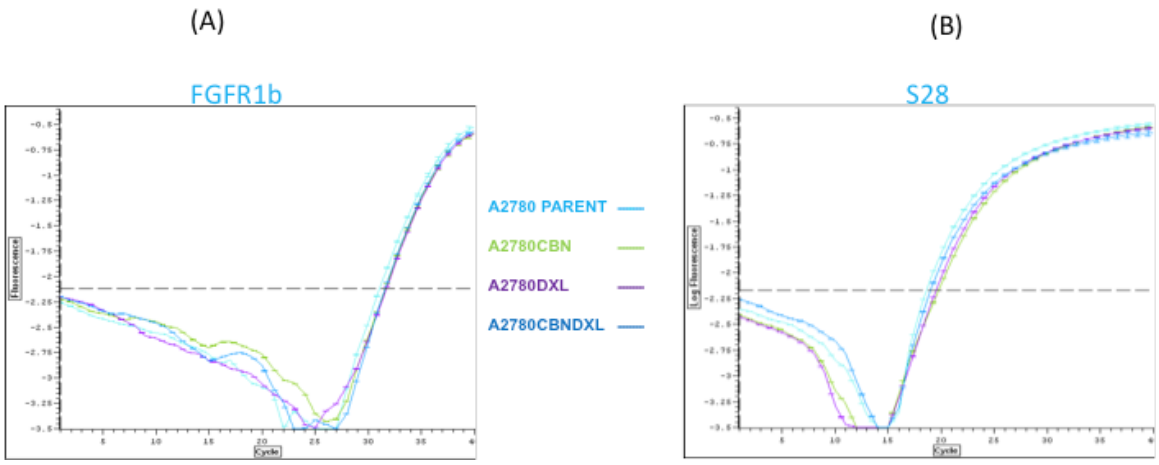

Figure 10: QPCR analysis of FGFR1b expression in the A2780 parent and resistant cell lines. (A) QPCR analysis for FGFR1b (B) QPCR for the S28 control in the A2780 parent and resistant cell lines.

The QPCR results for FGFR1c, FGFR2b and FGFR2c indicated that there was not any amplification seen in A2780CBN, A2780DXL and A2780CBNDXL resistant cell lines, meaning that there was no expression of these receptors in the A2780 cell lines (Figures 11 A, B, C).

Finally, the QPCR results for FGFR3 showed expression in all the A2780 cell lines but there was no difference seen between the A2780 parental cells and all three resistant cell lines (Figure 12, Table 5).

Based on the QPCR analyses, FGF18, FGF20 and FGF23 are the most interesting changes in FGF expression between the A2780 parent and resistant cell lines. Therefore, the protein expression level of these FGF factors will be validated using western blotting technique. As mentioned above, testing FGF18 is important because it involves in clusters analysis in two lines which are A2780CBN and A2780CBNDXL. However FGF20 is not involved in clusters but it has the biggest change that is present in the A2780CBNDXL cell line (-131.53). In addition, FGF23 is well known to be involved in epithelial ovarian cancer.

(A)

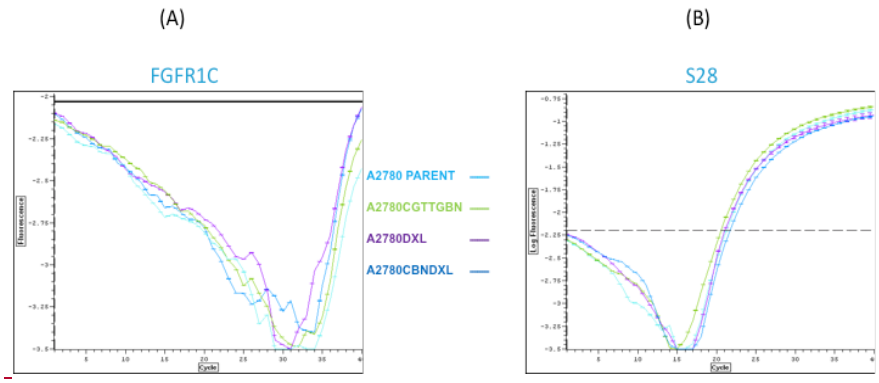

(B)

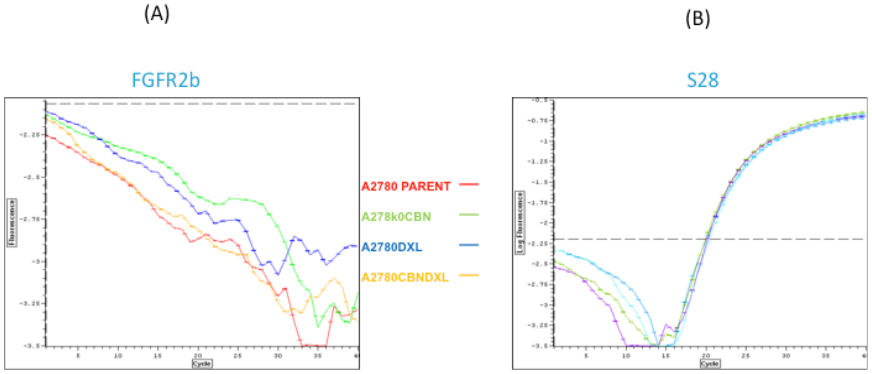

(C)

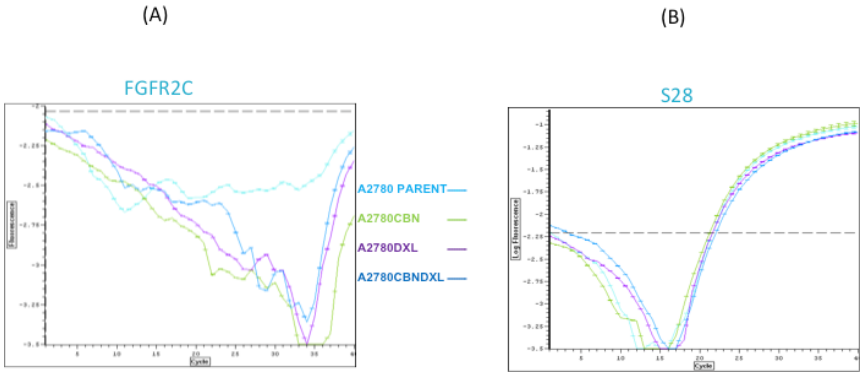

Figure 11 A, B, C: QPCR analysis of FGFR1c, FGFR2b and FGFR2c expression in the A2780 parent and resistant cell lines. (A) QPCR analysis for FGFR1c FGFR2b and FGFR2c. (B) QPCR for the S28 control in the A2780 parent and resistant cell lines.

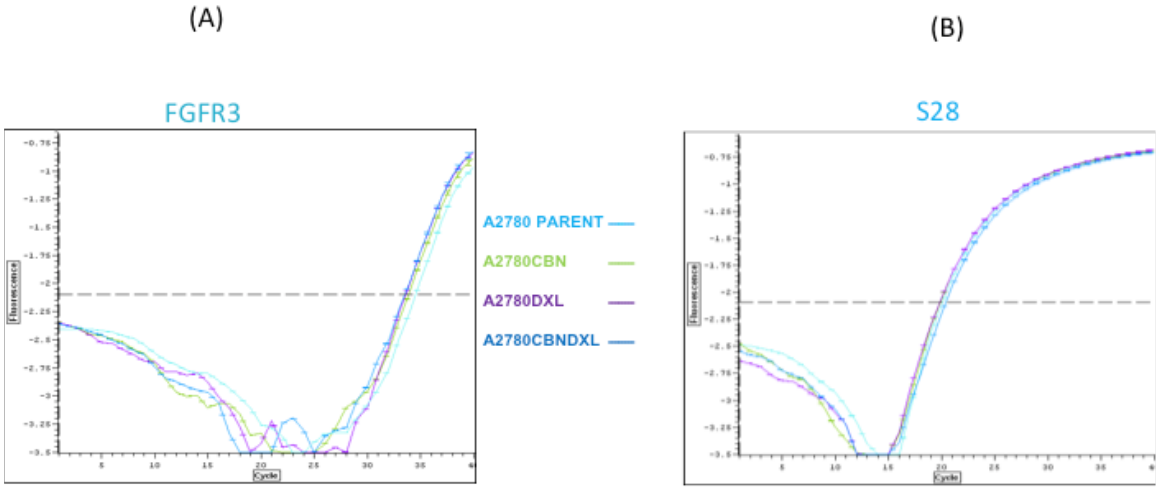

Figure 12: QPCR analysis of FGFR3 expression in the A2780 parent and resistant cell lines. (A) QPCR analysis for FGFR3. (B) QPCR for the S28 control in the A2780 parent and resistant cell lines.

Immunoblots to confirm protein expression of FGF factors

The immunoblots for FGF18, FGF20 and FGF23 were performed using two approaches to validate changes in protein expression confirmed by the QPCR analysis. One approach involved using cell lysates which would investigate the internal production of FGF factors and the second approach was to determine the presence of FGF in the culture medium which would investigate the secretion of FGF factors.

Immunoblots using cell lysates

The immunoblots for FGF18 were performed using an antibody that was supposed to detect FGF18 as a protein at about 23 kDa, which is an appropriate estimated mass for FGF18. Although no bands at about 23 kDa could be detected in the immunoblots, there was a band visible in the immunoblot at about 20 kDa as well as many non-specific bands. The band migrating at the 20 kDa size marker was the best candidate for the FGF18 protein (Figure 13A). Although the expression of FGF18 seems to be lower in the A2780CBNDXL cell line compared to the other cell lines, including the A2780 parent line, densitometry analysis of three biological replicate immunoblots did not confirm any significant difference in FGF 18 protein between any of the resistant cell lines and the parent A2780 cell line (Figure 13C). The loading control we have chosen was beta-actin which has a size of (37 KDa). The density of the beta-actin bands was used to normalize the density values of the FGF18 bands. Therefore, the immunoblots for FGF18 did not confirm the QPCR result and was not significantly down regulated in A2780CBN based on the antibody we have used (FGF18- abcam- ab86571).

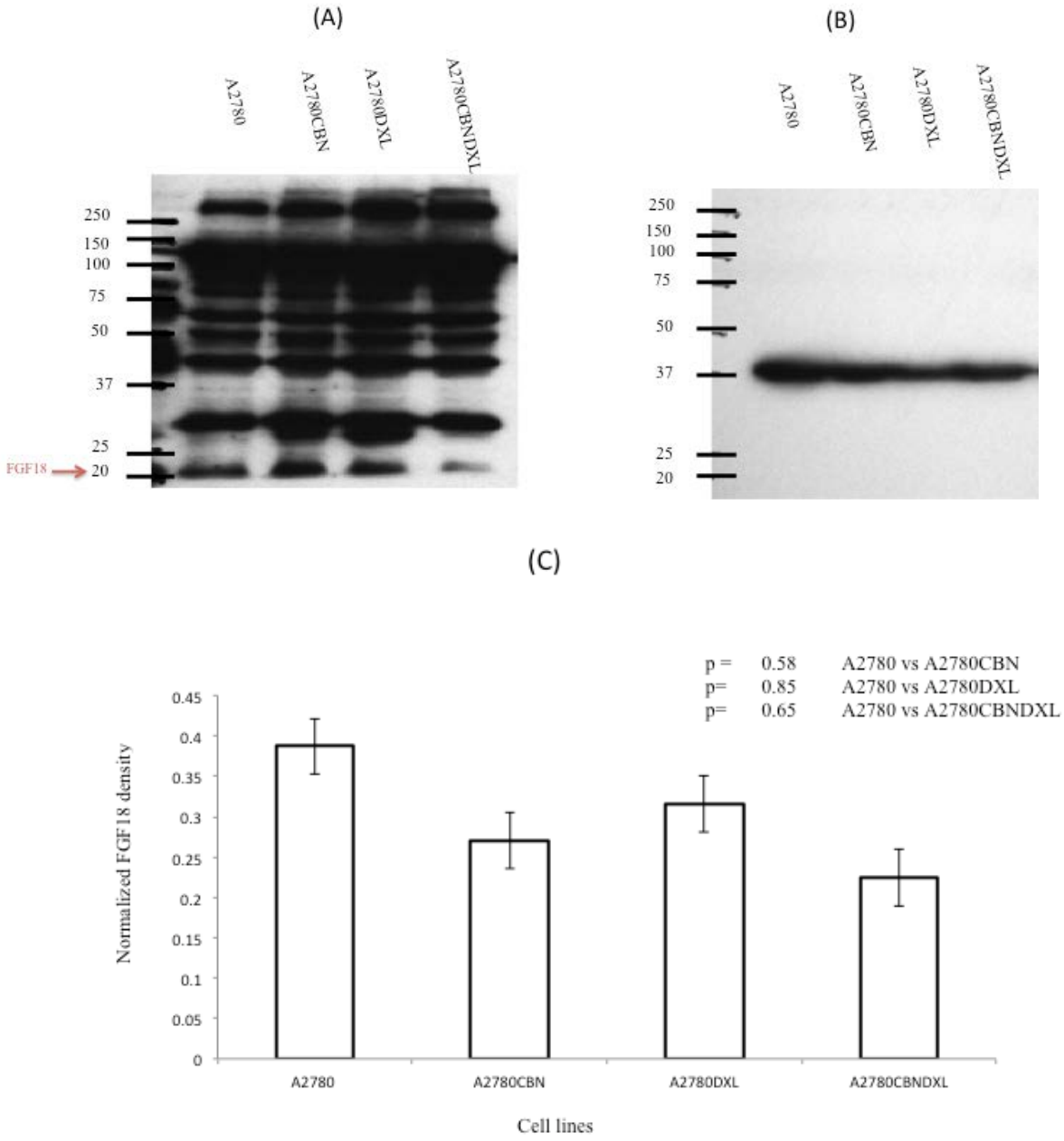

Figure 13: FGF18 immunoblot of protein lysates from the A2780 parent and resistant cell lines.(A)Immunoblot of the FGF18 protein., (B) Immunoblot of the beta-actin loading control (C) Densitometry measurement of FGF18 bands normalized to the beta-actin controls.

The FGF20 immunoblots were performed using an antibody to detect FGF20 at a mass of about 24 KDa and were done using cell lysates. While the immunoblots did not show FGF20 expression in the region of the 25 kDa marker, there were bands apparent in the region between the 25 and 37 kDa markers, migrating closer to 30 kDa marker (Figure 14A). There was a lack of non-specific bands in the immunoblots generated by this antibody, so the one band detected on the immunoblot was assumed to represent the FGF20 protein. Densitometry measurement of FGF20 immunoblot bands normalized to the beta-actin bands, did not show any significant differences between the parent cell line and the three resistance cell lines (Figure 14C). Therefore, the immunoblots for FGF20 did not confirm the QPCR result in that FGF20 was significantly down regulated in the A2780CBN or A2780CBNDXL cell lines based on the antibody we have used (FGF20-R&D system- AF2547).

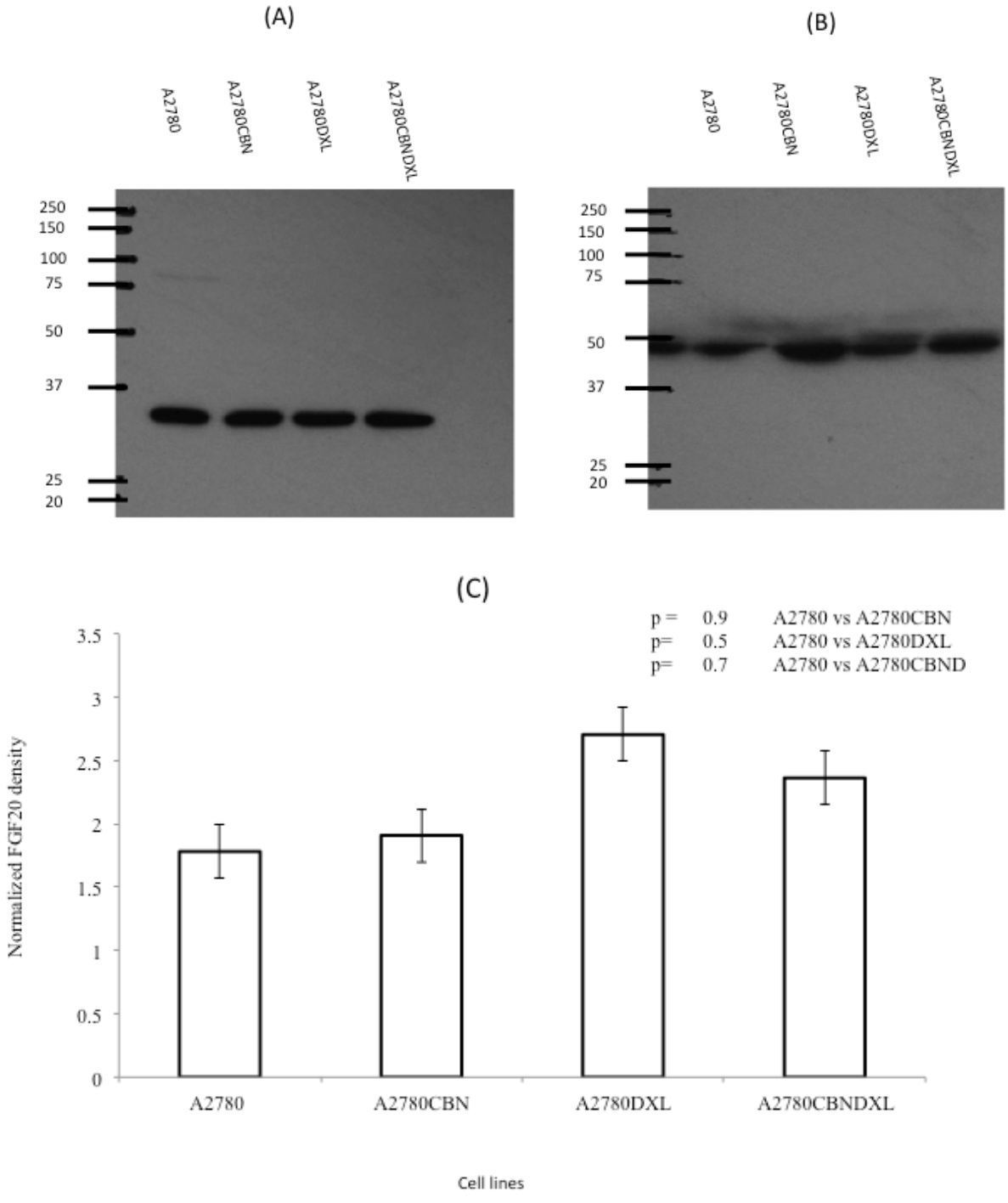
(A)
A2780
A2780CBN
A2780DXL
A2780CBNDXL
250
150
100
75
50
37
25
20
(B)
A2780
A2780CBN
A2780DXL
A2780CBNDXL
250
150
100
75
50
37
25
20
(C)
p = 0.9 A2780 vs A2780CBN
p= 0.5 A2780 vs A2780DXL
p= 0.7 A2780 vs A2780CBND
Normalized FGF20 density
3.5
3
2.5
2
1.5
1
0.5
0
A2780
A2780CBN
A2780DXL
A2780CBNDXL
Cell lines

Figure 14: FGF20 immunoblot of protein lysates from the A2780 parent and resistant cell lines. (A) Immunoblot of the FGF20 protein., (B)Immunoblot of the beta-actin protein in the A2780 parent and resistant cell lines.(C) Densitometry measurement of FGF20 bands normalized to the beta-actin controls.

The FGF23 immunoblots were performed using an antibody that was supposed to detect FGF23 at a mass of about 30-32 kDa. There were numerous non-specific bands in the immunoblots but around the 30 to 32 kDa region, a strong band was observed in the A2780 parent cell line, which was not seen in A2780CBN resistant cell line but was present in the A2780DXL and in the A2780CBNDXL resistant cell lines, although in the latter there appeared to be a lighter band (Figure 15A). Based on the mass of the band and the expression pattern in the cell lines, this band was assumed to represent the FGF23 protein. The densitometry measurement of the FGF23 immunoblot bands showed a significant reduction in the band density, normalized to beta-actin, in the A2780CBN and A2780CBNDXL resistant cell lines compared to the A2780 parent cell line. However, no difference was found between the A2780 parent cell line and the A2780DXL cell line in terms of FGF23 expression (Figure 15C). The immunoblots for FGF23 confirmed the QPCR result which showed significant downregulation of the FGF23 transcript in the A2780CBN and A2780CBNDXL resistant cell lines.

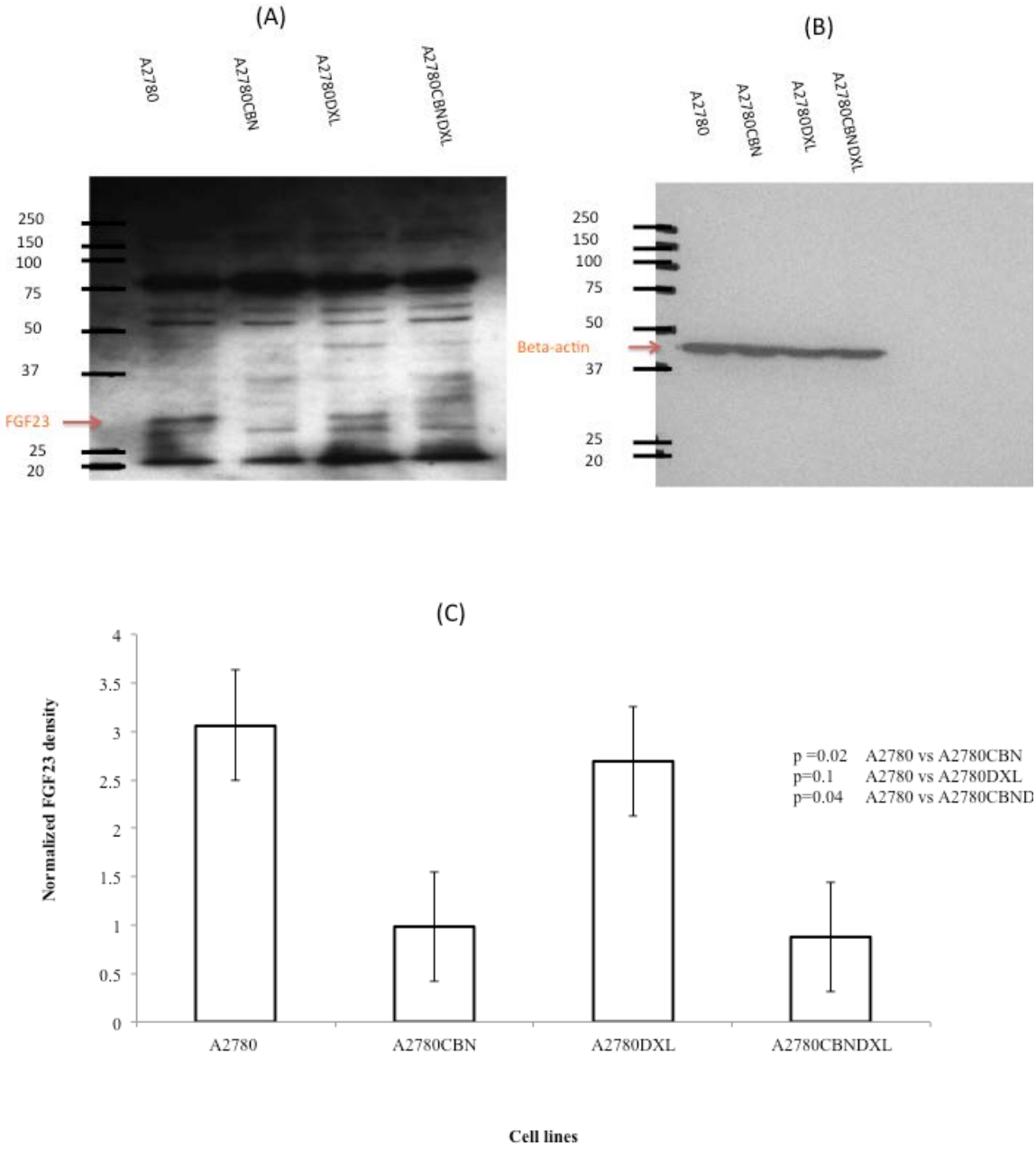

Figure 15: FGF23 immunoblot of protein lysates from the A2780 parent and resistant cell lines. (A) The FGF23 immunoblot. (B) Immunoblot of the beta-actin loading control in the A2780 parent and resistant lines (C) Densitometry measurement of FGF23 bands, normalized to beta-actin.

Immunoblots of culture supernatants

The FGF growth factors may be secreted and can have a paracrine or endocrine distribution. Both FGF18 and FGF20 have paracrine signaling and FGF23 is an endocrine factor. Since there is a possibility that the A2780 cell lines could be secreting the FGF factors, we decided to investigate if the FGF18, FGF20 and FGF23 factors could be detected in the cell culture supernatants and if the levels might be different for the resistant cell lines compared to the parent. To analyze the culture supernatants, culture medium was concentrated using Amicon centrifugal filter devices with a molecular weight cut-off of 50 kDa and 10 kDa. Equal amounts of protein from each concentrated culture supernatant were run on SDS-PAGE gels and transferred to membranes for immunoblotting. The same antibodies that were used for the cell lysate immunoblots were used for the culture supernatant immunoblots. The band patterns were very different for the culture supernatants compared to the cell lysates (Figure 16). Based on the expected band sizes for FGF18, FGF20 and FGF23, there was no expression of any of the three FGF factors observed in the immunoblots (Figure 16).

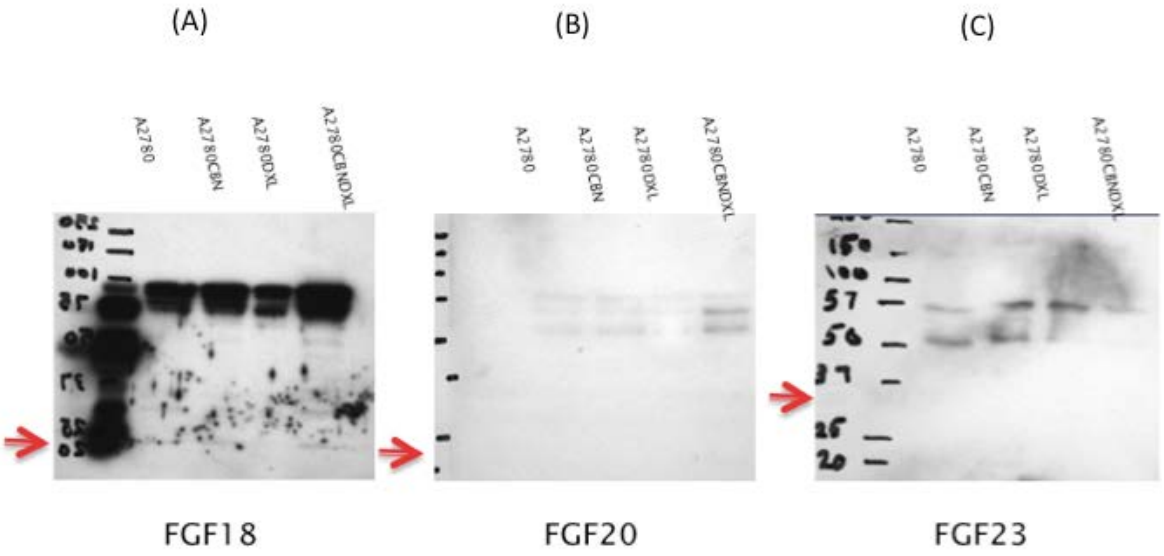

Figure16: Culture medium immunoblots for FGF18, FGF20 and FGF23.(A) Immunoblot for FGF18. (B) Immunoblot for FGF20. (C) Immunoblot for FGF23.

In summary, based on these results the immunoblots for FGF18 using cell lysate did not confirm the QPCR result and was not significantly down regulated in A2780CBN as well as the immunoblots for FGF20 did not confirm the QPCR result in that FGF20 was not significantly down regulated in the A2780CBN or A2780CBNDXL cell lines. Only FGF23 seems to be promising and confirmed the QPCR result which showed significant downregulation of the FGF23 transcript in the A2780CBN and A2780CBNDXL resistant cell lines. Additionally, immunoblots of culture supernatants did not show any expression of the three FGF factors.

Small interfering RNA (siRNA) to knockdown FGF23 expression

Based on the western blotting analysis FGF23 was the most interesting changed to knockdown, it was significantly down regulated in A2780CBN and A2780CBNDXL. To knockdown the promising gene, siRNA experiments was conducted under varying conditions. Experimental conditions were derived from the Ambion and Lifetechnologies handbook for siRNA and combined with the recommendations from the Lipofectamine protocol. These conditions included three transfection controls which were lipofectamine to test if Lipofectamine had a negative effect on the cells and the negative control-scrambled siRNA, to confirm that any siRNA transfection per se does not have a negative effect on the cells. In addition a positive control was planned, which was the housekeeping gene GAPDH, which was supposed to show that siRNA knockdown can be done successfully. To knock down the expression of FGF23, three Stealth siRNA were purchased from Life Technology/Ambion to test if single or pooled siRNA transfections will knockdown FGF23.

The QPCR analysis of GAPDH in A2780 cells that had been transfected for 24 hr with a Stealth GAPDH siRNA did not show any knockdown of GAPDH expression. There were not any differences between the negative control-scrambled siRNA and the three different concentrations for the GAPDH (50nM, 100nM and 200nM) (Figure 17) (Table 6).

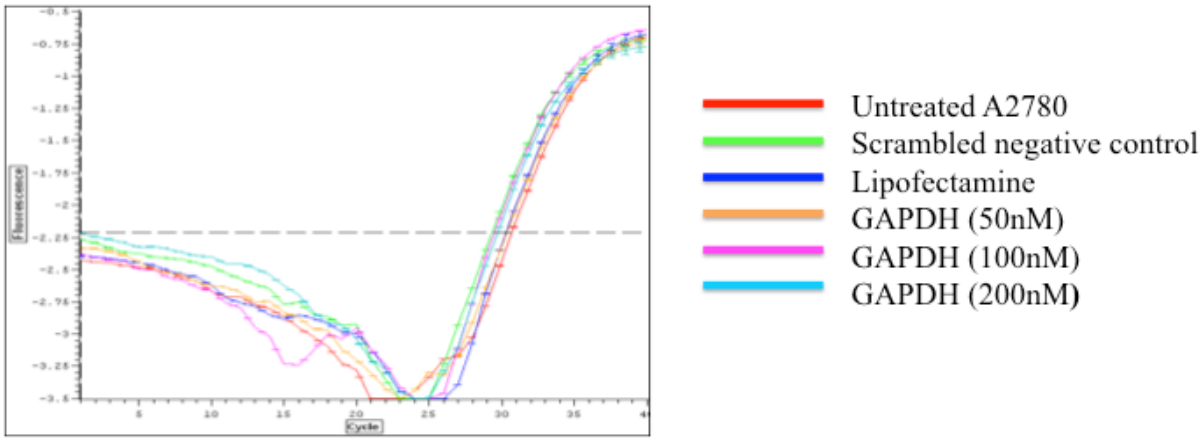

Figure 17: QPCR analysis for siRNA transfection for 24 hr GAPDH knockdown.

24 hr	Fold changes values	P values
GAPDH (50 nM)	1.0123	0.2828
GAPDH (100 nM)	1.0053	0.2579
GAPDH (200 nM)	1.0125	0.0753

Table 6: Fold change values and the P values based on the QPCR analysis of the 24 hr GAPDH siRNA experiments. The P values are calculated for each QPCR analysis comparing GAPDH (50nM, 100nM and 200 nM) to the negative control-scrambled siRNA.

A similar result was observed for the 48 hr transfections, the QPCR did not show any significant change between the scrambled negative control and the A2780 cells transfected with three different concentrations (50nM, 100nM and 200nM) of the GAPDH siRNA (Figure 18) (Table 7).

Block-IT Transfection experiments

The failure of the GAPDH knockdown experiment lead us to test if the A2780 cells were actually taking up siRNA, using lipofectamine in medium with or without serum. To do this, a Block-IT test oligo was purchased from Ambion. The Block-IT oligo is a nonsense oligo, not targeted to any known gene, and is fluorescently labeled. Block-IT oligos can be detected using FITC detection conditions.

The Block-IT transfection experiments were done using three different concentrations (10nM, 50nM and 100nM). We also used two different concentrations of lipofectamine which are (5µl and 10µl) to test whether the amount of lipofectamine was adequate, in addition to increasing the incubation times (24 hr, 48 hr and 72 hr). Of the three incubation times tested, the 48 hr transfection was performed in either RPMI with 10% FBS or low serum Optimem. For all transfections, the transfection medium containing the siRNA was changed to antibiotic-free medium after a 24 hr transfection incubation period (Table 8). Transfection efficiency was determined by counting the number of fluorescent cells and calculating the ratio between the total number of cells and the fluorescent cells.

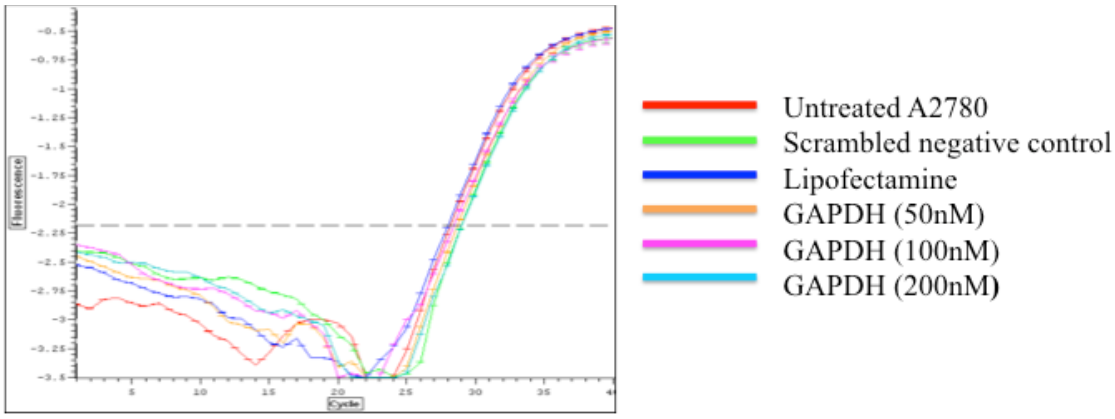

Figure 18: QPCR analysis for siRNA transfection for 48 hr GAPDH knockdown.

48 hr	Fold changes values	P values
GAPDH (50 nM)	0.9917	0.1975
GAPDH (100 nM)	0.9874	0.1021
GAPDH (200 nM)	1.0021	0.3875

Table 7: Fold change values and the P values based on the QPCR analysis of the 48 hr GAPDH siRNA experiments. The P values are calculated for each QPCR analysis comparing GAPDH (50nM, 100nM and 200 nM) to the negative control-scrambled siRNA.

The results for the 24 hr Block-IT transfection did not have high transfection values, likely because it was too early for the A2780 cells to show a significant difference in fluorescence (Appendix 1). The transfection efficiencies had a range of 50-60 %. The 48 hr Block-IT transfection produced reasonable results, which allowed us to count cells that had been successfully transfected. The transfection efficiency using Optimem in 10 and 50 nM with 5µl lipofectamine was higher than using RPMI with 10% FBS, also it was higher in 100 nM using 10µl lipofectamine. However, the 72 hr Block-IT transfection, A2780 cells were overgrown and was too difficult to count, therefore, no transfection efficiency values were calculated for the 72 hr transfections.

	5µl Lipofectamine		10µl Lipofectamine	
Block-IT concentration	RPMI 10% FBS	OPTIMEM	RPMI 10% FBS	OPTIMEM
0 nM	0%	0%	0%	0%
10 nM	30.3%	42.0%	71.1%	56.2%
50 nM	47.1%	72.8%	89.1%	61.5%
100 nM	76.9%	71.1%	72.4%	85.7%

Table 8: Transfection efficiency for the 48 hr Block-IT transfections with varying condition. Three different concentrations of Block-IT oligo were used (10 nM, 50 nM and 100 nM), two different concentrations of Lipofectamine (5µl and 10µl) were used and performed two different transfections in either Optimem or RPMI containing 10%FBS without antibiotic.

After the Block-IT experiments showed what the optimal conditions were for a successful transfection, we repeated the 48 hr GAPDH siRNA experiment using the optimal conditions from the Block-IT experiments and with fresh, newly purchased Stealth siRNA for GAPDH. For example, we used varying concentrations of (10 nM, 20 nM and 50 nM) siRNA, we also performed the transfections in Optimem and then removed transfection mixture from cells after 24 hr and replaced with fresh RPMI and 10%FBS without antibiotic. However, no significant difference was seen between the controls and the GAPDH. The S28 control QPCR reaction was used in this experiment to monitor the experimental conditions (Figure 19) (Table 9).

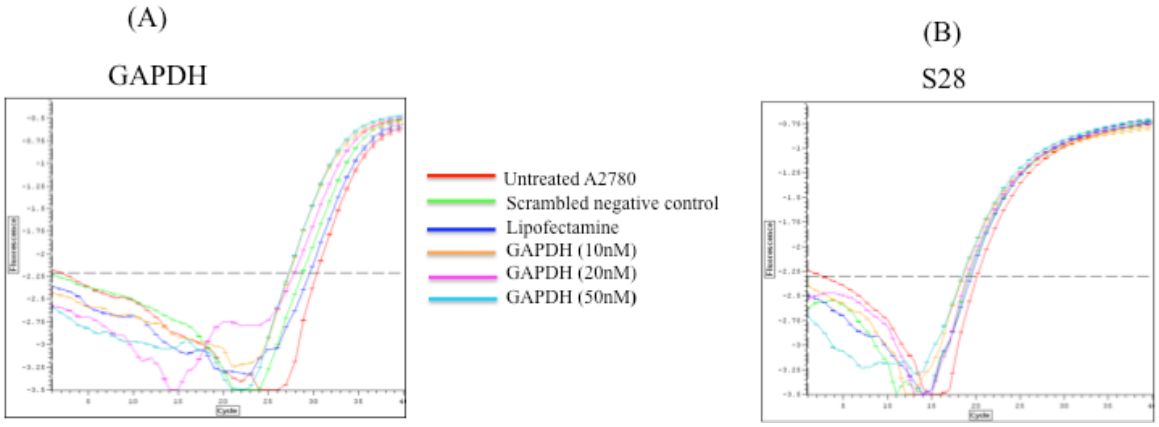

Figure 19: QPCR analysis for siRNA transfection for 48 hr GAPDH knockdown; (A) QPCR curves for the controls and the GAPDH with three different concentration (10 nM, 20 nM and 50 nM). (B) QPCR curves for the S28 control in the controls and the GAPDH siRNA treated samples.

	Fold changes values	P values
GAPDH (10 nM)	1.0475	0.0765
GAPDH (20 nM)	1.0261	0.0558
GAPDH (50 nM)	1.0034	0.0522

Table 9: Fold change values and the P values based on the QPCR analysis of the GAPDH siRNA experiments. The P values are calculated for each QPCR analysis comparing GAPDH (10nM, 20nM and 50 nM) to the negative control-scrambled siRNA.

After the failure of GAPDH knockdown experiments, we decided to discontinue the work with GAPDH siRNA and focus on testing the FGF23 siRNA. There were three different stealth FGF23 siRNA purchased from Ambion (HSS 111947, HSS 111948 and HSS 188481). We set up transfections for each FGF23 siRNA alone, and we also combined theFGF23 siRNA in pairs, in addition to setting up one transfection with all three FGF23 siRNA pooled. The controls were as before.

Starting with single FGF23 siRNA, there were not any significant changes seen between the controls and the single FGF23 siRNA with using 10nM (Figure 20) (Table 10).

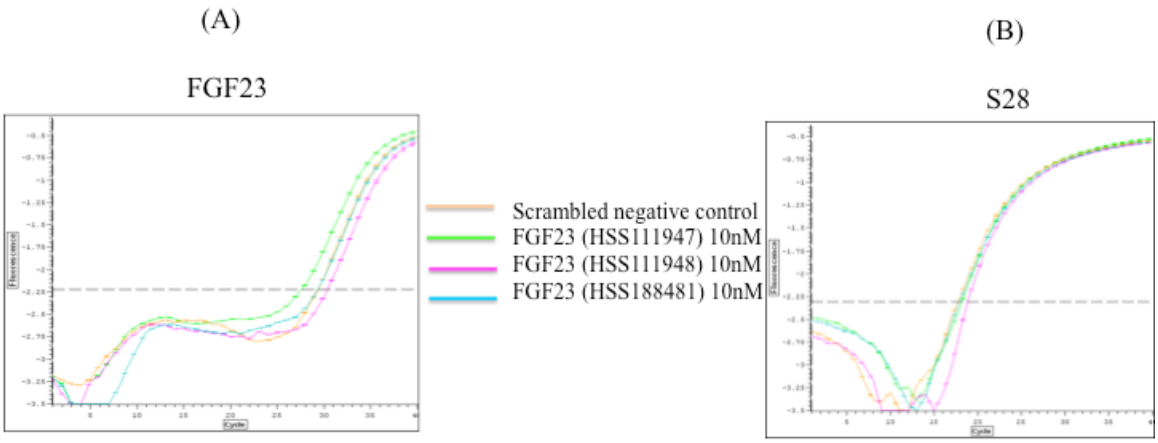

Figure 20: QPCR analysis for siRNA transfection for 48 hr single FGF23 knockdown. (A) Comparison of the scrambled negative control and the single FGF23 siRNA in 10 nM. (B) Shows the S28 control.

	Fold changes values	P values
FGF23 (HSS111947) 10nM	0.8779	0.1415
FGF23 (HSS111948) 10nM	0.8990	0.1604
FGF23 (HSS188481) 10nM	0.8855	0.1282
FGF23 (HSS111947) 20nM	0.8684	0.0982
FGF23 (HSS111948) 20nM	0.8912	0.1663
FGF23 (HSS188481) 20nM	0.9027	0.1700
FGF23 (HSS111947) 50nM	0.8356	0.5632
FGF23 (HSS111948) 50nM	0.9350	0.2773
FGF23 (HSS188481) 50nM	0.8905	0.1643

Table 10: the fold changes values and the P values based on the QPCR analysis. The P values are calculated for each QPCR analysis comparing single siRNA for FGF23 (10nM, 20nM and 50 nM) to the negative control-scrambled siRNA.

A similar observation was seen using a higher concentration of 20 nM FGF23 siRNA, there were no significant changes between the scrambled negative control and the three different siRNA (Figure 21) (Table 10).

Finally, with the highest concentration of FGF23 siRNA (50 nM), we still did not see any significant different between the scrambled negative control and the FGF23 siRNA knockdown samples (Figure 22) (Table 10).

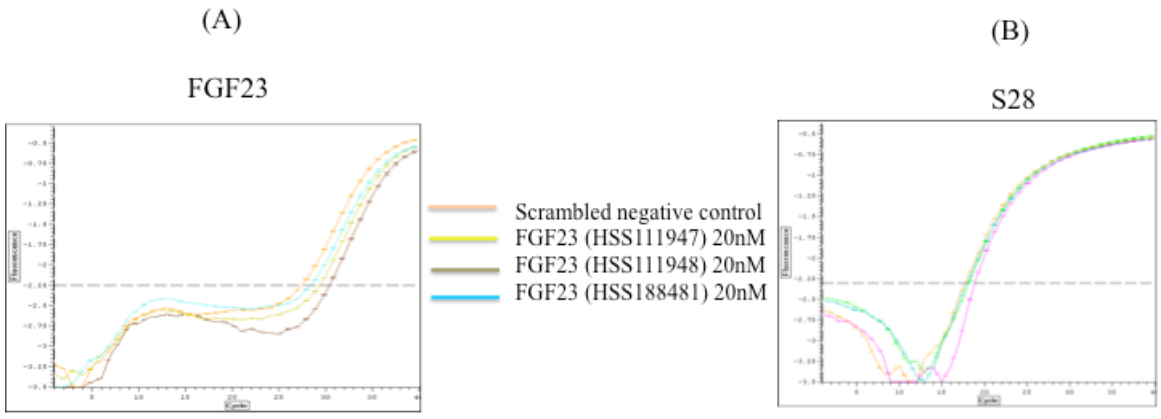

Figure 21: QPCR analysis for FGF23 siRNA transfection for 48 hr using single FGF23 siRNA. (A) QPCR curves for the scrambled negative control and the single FGF23 siRNA at a concentration of 20 nM. (B) QPCR curves for the S28 control in the control and the FGF23 single knock down samples.

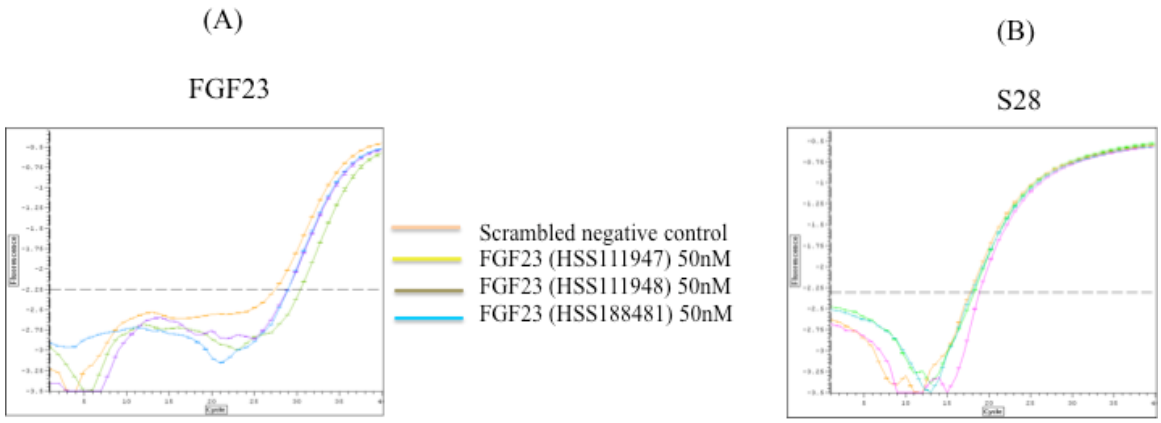

Figure 22: QPCR analysis for siRNA transfection for 48 hr single FGF23 knockdown. (A) QPCR curves for the scrambled negative control and the single FGF23 siRNA in 50 nM. (B) QPCR curves for the S28 control in the scrambled negative control and the FGF23 siRNA knockdown samples.

After that, all possible combinations of the FGF23 siRNAs were combined in pooled transfections. The combinations were as follows: (HSS 111947+ HSS 111948), (HSS 111947+ HSS 188481), (HSS 111948+ HSS 188481) and (HSS 111947+ HSS 111948+ HSS 188481). Despite combining the FGF23 siRNAs, no significant changes were seen between the scrambled negative control and the combined FGF23 siRNA samples (Figure 23) (Table 11).

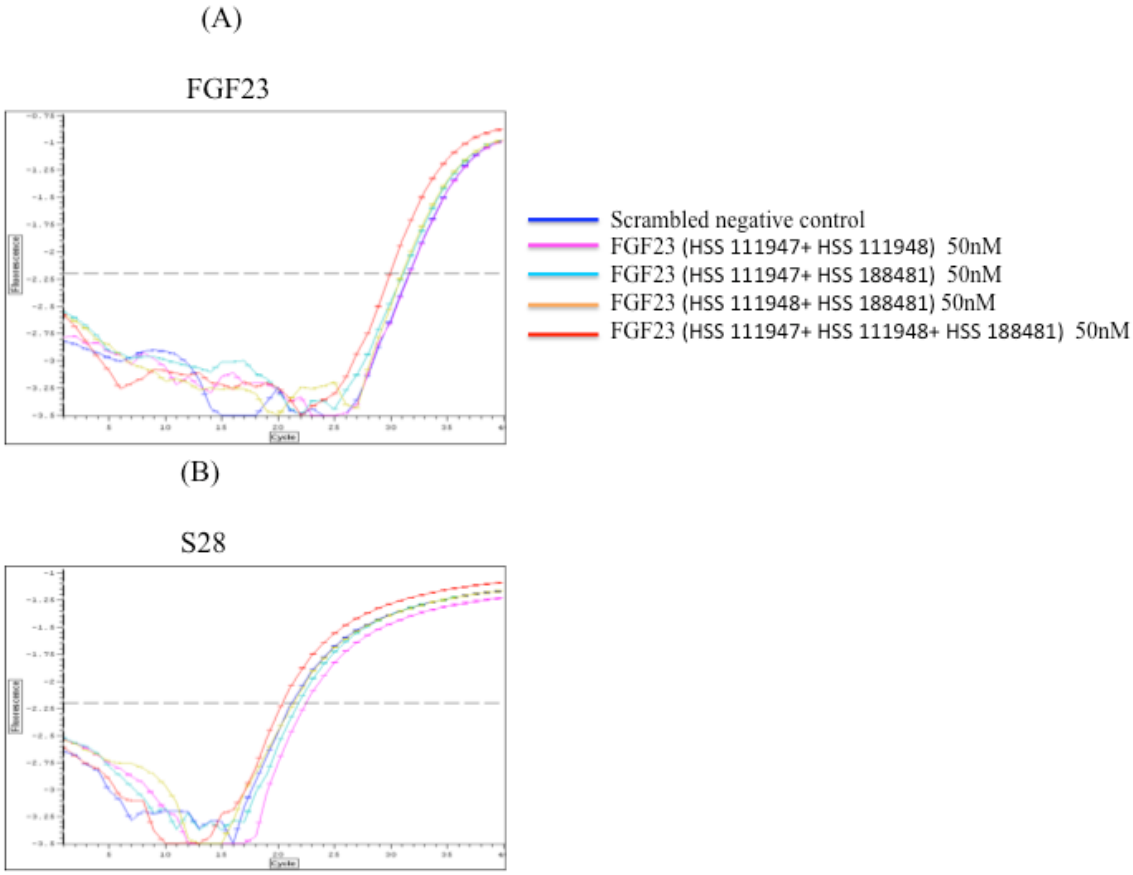

Figure 23: QPCR analysis for siRNA transfection for 48 hr pooled FGF23 knockdown. (A) Comparison of the scrambled negative control and the single FGF23 siRNA in 50 nM. (B) Shows the S28 control.

	Fold changes values	P values
FGF23 (HSS111947+HSS111948) 50nM	1.0521	0.0573
FGF23 (HSS111947+HSS188481) 50nM	1.0231	0.0645
FGF23 (HSS111948+HSS188481) 50nM	1.0038	0.4324
FGF23 (HSS111947+HSS111948+HSS188481) 50nM	0.9917	0.2318

Table 11: the fold changes values and the P values based on the QPCR analysis. The P values are calculated for each QPCR analysis comparing pooled siRNA for FGF23 (50 nM) to the negative control-scrambled siRNA.

Discussion

Based on the previous work done by Armstrong *et al.* and the FIN analysis performed by Dr. Kalatskaya of the OICR, there were indications that changes in the expression of FGF genes could contribute to the development of resistance to chemotherapy drugs in ovarian cancer cells. The hypothesis for the current study was that changes in FGF gene expression contributed to the development of resistance to carboplatin, docetaxel and combined carboplatin/docetaxel in A2780 ovarian cancer cells. Of the FGF genes found to have changes in gene expression in the drug resistant cell lines developed by Armstrong *et al.,* QPCR analysis could only show significant changes in mRNA transcripts in FGF18, FGF20 and FGF23 in the three resistant cell lines compared to the A2780 parent cells. However, we could only confirm a change in protein expression for FGF23, which was shown to be altered in A2780CBN and A2780CBNDXL cells compared to the A2780 parent cells. Since a change in expression could only be shown for the FGF23 gene, siRNA experiments were performed to attempt to knockdown its expression in the A2780 parent cell line, in order to determine if changing the expression of the FGF23 induce drug resistance in the A2780 parent cell line. Unfortunately, the knockdown of FGF23 in the A2780 cell line was not successful using the siRNA technique, so no firm conclusions can be drawn regarding the role of FGF23 in the development of drug resistance in ovarian cancer cells.

Numerous studies have reported changes in the expression of FGFs or their receptors associated with the development of different types of ovarian cancer. The FGFs can

play a role in demethylation of other genes which may lead to the development of cancer [77]. However, many of the changes in FGF levels have been observed in the high grade serous (HGS) type of ovarian cancer and the A2780 cell line is of the endometrioid type. Some of the first studies reported changes in FGF2 (basic FGF) expression levels in ovarian tumors [78, 79]. Later studies detected changes in other FGF factors, for example FGF1, FGF20, FGF23 and FGFR3 associated with several forms of ovarian cancer such as the HGS, endometrioid, and clear cell subtypes [70, 75, 80-82]. As progress was made in ovarian cancer research, evidence for the involvement of FGF factors in response and resistance to chemotherapy was found [71, 76, 83-85]. In these studies, several FGF factors and FGF receptors were surveyed for expression changes in drug resistant A2780 cell lines, including FGF1, FGF2, FGF18, FGF20, FGF23, FGFR1, FGFR2 and FGFR3. Despite the evidence for involvement of FGF1, FGF2, FGFR1, FGFR2 and FGFR3 in drug resistance [71, 76, 84], only transcripts of FGF18, FGF20 and FGF23 were seen to be altered in the A2780 resistant cell lines based on the QPCR analysis. This was an expected result for FGF20, since it has been shown to be upregulated in the A2780 cell line compared to a non-cancerous cell line [86]. FGF18 also is known to be prognostic and therapeutic biomarker in epithelial ovarian cancer regards to amplification of chromosomal region 5q31-5q35.3 which has been found to predict poor prognosis in patients with advanced stage and the overexpression of FGF18 is also a marker that promote tumor progression [68]. Therefore, it would be possible to see changes in FGF18 since FGF18 makes cancer cells grow faster and the drug resistant cell lines are known to grow slower then knocking down FGF18 would slow the growth of

cancer cells. However, some FGF factors were seen to be altered in other ovarian cancer cell lines but were not seen to be changed in the A2780 cell line for example FGF1, FGF2 and FGFR3 were seen to be different in the HGS cell lines [84, 87, 88]. FGFR1 also has been shown to be altered in the SKOV3 cell line relative to normal cells [76]. Therefore, we would not expect them to necessarily be changed in our resistant cell line A2780.

In addition, we would not expect all FGF factors that were identified as having altered expression in our drug-resistant cell lines relative to their co-cultured controls by microarray analysis to be true changes, because it is known that microarray is not high quantitative, in particular for poorly-expressed genes. However, QPCR analysis is more accurate since the primers were designed to be specific for the gene transcripts. Therefore, it would be possible to see changes in the microarray which are not necessarily confirmed by QPCR. For example, QPCR showed a dramatic change of the FGF23 transcript in the A2780CBN (-22.5 fold change), however the microarray showed no expression. FGF18 also showed upregulation in A2780CBNDXL in the microarray results, but the QPCR results showed downregulation since the Q-PCR is much more quantitative and has high sensitivity and specificity to detect a transcript

The immunoblots for FGF23 using cell lysates confirmed the QPCR results, which showed significant downregulation of the FGF23 transcript in the A2780CBN and A2780CBNDXL drug-resistant cell lines. It also confirmed the microarray result,

which showed a significant downregulation of the FGF23 transcript in A2780CBNDXL cells.

The result from the FGF18 immunoblotting experiments did not confirm the QPCR results, which showed a downregulation of the FGF18 transcript in the A2780CBN cell line relative to A2780 cells, it also did not confirm the microarray result which showed an upregulation of the FGF18 transcript in the A2780CBNDXL cell line relative to A2780 cells. The FGF18 immunoblots showed many non-specific bands but the band that represents FGF18 protein is most likely to be around 20 KDa. Densitometry measurements of the FGF18 immunoblot bands normalized to the beta actin bands did not show a significant difference in FGF18 protein levels between the A2780 parent cells and the three resistant cell lines. Therefore, the protein result did not confirm either the microarray or the QPCR result; rather, it showed a very different result. We expected to see a downregulation in FGF18 protein levels in A2780CBN cells based on our QPCR findings (-8.9); however, these changes were not observed in the FGF18 immunoblots. While microarray studies suggested an upregulation of about 7- fold in FGF18 transcript levels in A2780CBNDXL cells, quantitative PCR findings suggested no change in FGF18 transcript levels in A2780CBNDXL cells. The immunoblot experiments confirm this lack of upregulation in A2780CBNDXL cells. Based on the immunoblot anlaysis of the FGF18 protein expression in the A2780 and drug resistant cell lines there were no significant differences in FGF18 expression in any of the drug resistant cell lines.

The FGF20 immunoblots that were performed did not show any bands in the region of the 25 KDa marker, which is the molecular weight of FGF20; rather, the bands were in the region between the 25 KDa and 37 KDa markers. It is possible that the FGF20 protein is post-translationally modified, perhaps by being glycosylated or phosphorylated. This would change the migration of the protein in the gel. Therefore, since the position of the FGF20 band is in a different region on the gel but there is only one clear band detected on the immunoblot, it is highly possible that this band represents the FGF20 protein. Unfortunately, densitometry measurement of FGF20 immunoblot bands normalized to the beta-actin bands, did not show any significant differences in relative FGF20 protein levels between the A2780 parent cell line and the three resistance cell lines. This is despite the dramatic changes in FGF20 expression that we detected by both QPCR and microarray analysis. However, it is possible for changes in mRNA levels to not correspond to the protein level due to regulation of mRNA levels between transcription and translation. For example natural RNAi can prevent translation of the transcript or alternative splicing can generate different transcripts that do not produce protein.
As a result, we can see mRNA highly upregulated but that does not always reflect the protein level.

The FGF18 and FGF20 immunoblots did not confirm either the QPCR or the microarray results, however if we had seen a result in protein expression that

corresponded to the QPCR or the microarray result that would mean they could play a role in drug resistance.

FGF18, FGF20 and FGF23 are members of different families, FGF18 is in family 8 and FGF20 is in family 9. Both families have a paracrine effect in target cells that is close to the cells producing the hormones. While FGF20 exhibited a major change in gene expression in drug-resistant cells, it is not clear how it could have an effect on drug resistance. FGF20 has been found to signal mainly through FGFR2b, FGFR2c, and FGFR3c in mouse fibroblasts, through FGFR1c in dopaminergic neurons and strongly through FGFR3b in binding assays in BaF3 cells [89-91]. However, in A2780 cells, only FGFR1b and FGFR3 were found to be expressed in our study and the primers used did not distinguish between isoforms of FGFR3 (Figure 10 and 12). Since only FGFR3 was detected in the A2780 cells and this type of signaling has been reported in mouse fibroblasts and in a binding assay in BaF3 cells, the connection to drug resistance in ovarian cancer is not immediately evident. One connection of FGFR3 to acquired resistance in myeloma cells has been reported, where a mutation in FGFR3 conferred resistance to FGFR inhibitors [92]. FGF23 belongs to the FGF19 subfamily which contains the FGF factors with an endocrine effect which can enter the blood circulation directly and disperse more than the rest of the FGF factors [55], which might have an impact on drug resistance by binding to FGF receptors in tumours throughout the body. In contrast to FGF20, FGF23 activates c-isoform receptors like FGFR1c, FGFR2c, FGFR3c and also FGFR4 [91]. Of these only FGFR3 was found to be expressed in A2780 cells, and as mentioned before, specific isoforms of FGFR3 were not distinguished in this study.

Nevertheless, the expression of FGFR3 does indicate that FGF23 signaling can occur in the A2780 cells. To date, the over expression of FGF23 in cancer has been shown to be associated with dysregulated serum phosphate levels, usually hypophosphatemia [55, 70], and there is no reported evidence of an association of FGF23 with drug resistance, other than the role of FGFR3 in acquired resistance to FGFR inhibitors as described. Although the signaling by both FGF20 and FGF23 through isoforms of FGFR3 might indicate a role for FGFR3 in these drug resistant cell lines, the report by Chell et al. focuses on loss of inhibition by FGFR inhibitors. This is in contast to resistance to carboplatin and combined carboplatin and docetaxel in A2780CBN and A2780CBNDXL cells, respectively, where changes in the expression of FGF20 and FGF23 occur, which might impact on FGFR3 signaling. .However, this does not preclude some other role for signaling through FGFR3 in resistance to carboplatin or carboplatin/docetaxel.

Since there is a possibility that the A2780 cell line could secret the FGF factors, we attempted to detect FGF secretion into the cell culture medium with the method of using Amicon centrifugation devices to concentrate the culture medium, with subsequent immunoblotting experiments with antibodies to the three FGFs having altered expression in our studies. None of the immunoblotting experiments were able to detect expression one or more of the three FGFs in the medium of our drug-resistant A2780 cells (Figure 16). The lack of detection of FGFs in the culture media may not be due to a lack of secretion of the factors but due to low levels of secretion

of FGFs, which were not adequately concentrated by the centrifugation method in our study to detect them.

A knockdown of FGF23 expression was not achieved in our experiments employing either the single siRNA against FGF23 or pooled siRNAs against FGF23. No significant difference in FGF23 transcript was observed between the A2780 parent cells and the three resistant cell lines. Since FGF23 was downregulated in the A2780CBN and A2780CBNDXL cell lines based on our immunoblot experiments, we would expect to see the A2780 parent cell line acquire resistance to CBN and/or DXL, if we had been successful in knocking down FGF23 transcript and protein expression in the A2780 cell line. If such a knockdown would have been possible, and the A2780 cells acquired resistant to carboplatin and/or DXL, then this would confirm FGF23's important role in carboplatin resistance.

One reason for the unsuccessful knockdown experiments may have been the poor level of cell transfection, due to a low transfection efficiency. However, we are fairly confident that the transfections were highly successful, given our findings with the BLOCK-iT transfection optimization experiments, which showed transfection efficiencies as high as 70-85%. Using the same conditions for both the GAPDH and FGF23 transfections did not, however, result in a significant knockdown in either GAPDH or FGF23 expression. Since it is unlikely that a low transfection efficiency was responsible for the lack of gene knockdown, other factors may have caused the failure of these experiments. For example, it is possible that the mRNA for FGF23 in

the A2780 cells has small genetic variations, which do not allow the siRNAs to bind effectively to the mRNA for FGF23. Since the siRNAs are only 21 nucleotides in length, any sequence change in the transcript could disrupt the binding of the siRNA. Another possibility is that the target for the siRNA, while binding to the transcript, did not result in targeted mRNA degradation. Targeting different areas within the transcript might have been needed.

We also had a similar expectation of induced drug resistance, if we had attempted and succeeded in knocking down FGF18 and FGF20 gene expression in A2780 cells. Moreover, if knockdown of all three FGF transcripts had a partial effect on drug resistance, then pooling them might have conferred even greater drug resistance.

Conclusion

We have been able to confirm some changes in gene expression from microarray and FIN analysis, suggesting a possible role for FGF in drug resistance. However, we could only confirm a change in protein expression for one of the FGF factors, which had reduced expression in A2780CBN and A2780CBNDXL cells.

Future directions

Future directions might involve repeating western blots with other antibodies to FGF20 and FGF18 (in order to possibly confirm changes in gene expression at the protein level). Repeating the siRNA knock down experiments for FGF23 using other siRNAs, targeted to other sites in transcript. CRISPR constructs may also be more

ideal for successfully knocking down FGF23 expression. Depending upon whether the future Western blots for FGF18 and FGF20 show consistent changes in protein expression in the drug resistant cell lines, then additional siRNA knockdown experiments for FGF18 and FGF20 could prove successful in drawing a further link between changes in FGF signalling pathways and drug resistance. In addition, it would be interesting to screen other data sets such as the Cancer Cell Line Encyclopedia (CCLE) to validate the result. This will allow us to identify a role for FGF growth factors as therapeutic targets in ovarian cancer.

References

1. Armstrong, S.R., et al., *Distinct genetic alterations occur in ovarian tumor cells selected for combined resistance to carboplatin and docetaxel.* J Ovarian Res, 2012. **5**(1): p. 40.
2. *Cancer statistics at a glance*.
3. *American Cancer Society.* 2015.
4. in *Referral Guidelines for Suspected Cancer in Adults and Children*. 2005: London (UK).
5. Goff, B.A., et al., *Development of an ovarian cancer symptom index: possibilities for earlier detection.* Cancer, 2007. **109**(2): p. 221-7.
6. Meyer, T. and G.J. Rustin, *Role of tumour markers in monitoring epithelial ovarian cancer.* Br J Cancer, 2000. **82**(9): p. 1535-8.
7. Cho, K.R. and M. Shih Ie, *Ovarian cancer.* Annu Rev Pathol, 2009. **4**: p. 287-313.
8. Prat, J., *New insights into ovarian cancer pathology.* Ann Oncol, 2012. **23 Suppl 10**: p. x111-7.
9. Cancer Genome Atlas Research, N., *Integrated genomic analyses of ovarian carcinoma.* Nature, 2011. **474**(7353): p. 609-15.
10. Gilks, C.B., *Molecular abnormalities in ovarian cancer subtypes other than high-grade serous carcinoma.* J Oncol, 2010. **2010**: p. 740968.
11. Gershenson, D.M., *The life and times of low-grade serous carcinoma of the ovary.* Am Soc Clin Oncol Educ Book, 2013.
12. Gemignani, M.L., et al., *Role of KRAS and BRAF gene mutations in mucinous ovarian carcinoma.* Gynecol Oncol, 2003. **90**(2): p. 378-81.
13. Ray, M. and G. Fleming, *Management of advanced-stage and recurrent endometrial cancer.* Semin Oncol, 2009. **36**(2): p. 145-54.
14. McConechy, M.K., et al., *Ovarian and endometrial endometrioid carcinomas have distinct CTNNB1 and PTEN mutation profiles.* Mod Pathol, 2014. **27**(1): p. 128-34.
15. Kumar, A., et al., *Patterns of spread of clear cell ovarian cancer: Case report and case series.* Gynecol Oncol Case Rep, 2013. **6**: p. 25-7.
16. Gounaris, I. and J.D. Brenton, *Molecular pathogenesis of ovarian clear cell carcinoma.* Future Oncol, 2015. **11**(9): p. 1389-405.
17. Beall, H.D. and S.I. Winski, *Mechanisms of action of quinone-containing alkylating agents. I: NQO1-directed drug development.* Front Biosci, 2000. **5**: p. D639-48.
18. Markman, M., *Antineoplastic agents in the management of ovarian cancer: current status and emerging therapeutic strategies.* Trends Pharmacol Sci, 2008. **29**(10): p. 515-9.
19. Zylberberg, B., et al., *Chemotherapy by the intravenous and intraperitoneal routes combined in ovarian cancer.* Gynecol Oncol, 1990. **36**(2): p. 271-6.

20. Tewari, D., et al., *Long-term survival advantage and prognostic factors associated with intraperitoneal chemotherapy treatment in advanced ovarian cancer: a gynecologic oncology group study.* J Clin Oncol, 2015. **33**(13): p. 1460-6.
21. Fung-Kee-Fung, M., et al., *Intraperitoneal chemotherapy for patients with advanced ovarian cancer: a review of the evidence and standards for the delivery of care.* Gynecol Oncol, 2007. **105**(3): p. 747-56.
22. Zeimet, A.G., et al., *Pros and cons of intraperitoneal chemotherapy in the treatment of epithelial ovarian cancer.* Anticancer Res, 2009. **29**(7): p. 2803-8.
23. Yap, T.A., C.P. Carden, and S.B. Kaye, *Beyond chemotherapy: targeted therapies in ovarian cancer.* Nat Rev Cancer, 2009. **9**(3): p. 167-81.
24. Lister-Sharp, D., et al., *A rapid and systematic review of the effectiveness and cost-effectiveness of the taxanes used in the treatment of advanced breast and ovarian cancer.* Health Technol Assess, 2000. **4**(17): p. 1-113.
25. Rabik, C.A. and M.E. Dolan, *Molecular mechanisms of resistance and toxicity associated with platinating agents.* Cancer Treat Rev, 2007. **33**(1): p. 9-23.
26. Rybak, L.P., et al., *Mechanisms of cisplatin-induced ototoxicity and prevention.* Hear Res, 2007. **226**(1-2): p. 157-67.
27. Marullo, R., et al., *Cisplatin induces a mitochondrial-ROS response that contributes to cytotoxicity depending on mitochondrial redox status and bioenergetic functions.* PLoS One, 2013. **8**(11): p. e81162.
28. Rowinsky, E.K., *The development and clinical utility of the taxane class of antimicrotubule chemotherapy agents.* Annu Rev Med, 1997. **48**: p. 353-74.
29. Davis, W., Jr., Z. Ronai, and K.D. Tew, *Cellular thiols and reactive oxygen species in drug-induced apoptosis.* J Pharmacol Exp Ther, 2001. **296**(1): p. 1-6.
30. Ciarimboli, G., *Membrane transporters as mediators of Cisplatin effects and side effects.* Scientifica (Cairo), 2012. **2012**: p. 473829.
31. Holzer, A.K., G.H. Manorek, and S.B. Howell, *Contribution of the major copper influx transporter CTR1 to the cellular accumulation of cisplatin, carboplatin, and oxaliplatin.* Mol Pharmacol, 2006. **70**(4): p. 1390-4.
32. Lin, X., et al., *The copper transporter CTR1 regulates cisplatin uptake in Saccharomyces cerevisiae.* Mol Pharmacol, 2002. **62**(5): p. 1154-9.
33. Ishida, S., et al., *Uptake of the anticancer drug cisplatin mediated by the copper transporter Ctr1 in yeast and mammals.* Proc Natl Acad Sci U S A, 2002. **99**(22): p. 14298-302.
34. Martinez-Balibrea, E., et al., *Increased levels of copper efflux transporter ATP7B are associated with poor outcome in colorectal cancer patients receiving oxaliplatin-based chemotherapy.* Int J Cancer, 2009. **124**(12): p. 2905-10.
35. Martin, L.P., T.C. Hamilton, and R.J. Schilder, *Platinum resistance: the role of DNA repair pathways.* Clin Cancer Res, 2008. **14**(5): p. 1291-5.
36. Fonseca, G., *Carboplatin: molecular mechanisms of action associated with chemoresistance.* Brazilian Journal of Pharmaceutical Sciences, 2014. **50**.
37. Fink, D., et al., *The role of DNA mismatch repair in platinum drug resistance.* Cancer Res, 1996. **56**(21): p. 4881-6.

38. Gascoigne, K.E. and S.S. Taylor, *How do anti-mitotic drugs kill cancer cells?* J Cell Sci, 2009. **122**(Pt 15): p. 2579-85.
39. Katsetos, C.D. and P. Draber, *Tubulins as therapeutic targets in cancer: from bench to bedside.* Curr Pharm Des, 2012. **18**(19): p. 2778-92.
40. Borst, P. and A.H. Schinkel, *P-glycoprotein ABCB1: a major player in drug handling by mammals.* J Clin Invest, 2013. **123**(10): p. 4131-3.
41. Ehrlichova, M., et al., *Transport and cytotoxicity of paclitaxel, docetaxel, and novel taxanes in human breast cancer cells.* Naunyn Schmiedebergs Arch Pharmacol, 2005. **372**(1): p. 95-105.
42. Hembruff, S.L., et al., *Role of drug transporters and drug accumulation in the temporal acquisition of drug resistance.* BMC Cancer, 2008. **8**: p. 318.
43. McFadyen, M.C., et al., *Cytochrome P450 CYP1B1 protein expression: a novel mechanism of anticancer drug resistance.* Biochem Pharmacol, 2001. **62**(2): p. 207-12.
44. Rodriguez-Antona, C. and M. Ingelman-Sundberg, *Cytochrome P450 pharmacogenetics and cancer.* Oncogene, 2006. **25**(11): p. 1679-91.
45. Kavallaris, M., et al., *Taxol-resistant epithelial ovarian tumors are associated with altered expression of specific beta-tubulin isotypes.* J Clin Invest, 1997. **100**(5): p. 1282-93.
46. Yin, S., R. Bhattacharya, and F. Cabral, *Human mutations that confer paclitaxel resistance.* Mol Cancer Ther, 2010. **9**(2): p. 327-35.
47. Tredan, O., et al., *Drug resistance and the solid tumor microenvironment.* J Natl Cancer Inst, 2007. **99**(19): p. 1441-54.
48. Williams, S.A., et al., *Patient-derived xenografts, the cancer stem cell paradigm, and cancer pathobiology in the 21st century.* Lab Invest, 2013. **93**(9): p. 970-82.
49. Johnson, S.W., R.F. Ozols, and T.C. Hamilton, *Mechanisms of drug resistance in ovarian cancer.* Cancer, 1993. **71**(2 Suppl): p. 644-9.
50. Rose, P.G. and M. Smrekar, *Improvement of paclitaxel-induced neuropathy by substitution of docetaxel for paclitaxel.* Gynecol Oncol, 2003. **91**(2): p. 423-5.
51. Hegde, P., et al., *A concise guide to cDNA microarray analysis.* Biotechniques, 2000. **29**(3): p. 548-50, 552-4, 556 passim.
52. Chon, H.S. and J.M. Lancaster, *Microarray-based gene expression studies in ovarian cancer.* Cancer Control, 2011. **18**(1): p. 8-15.
53. Russo, G., C. Zegar, and A. Giordano, *Advantages and limitations of microarray technology in human cancer.* Oncogene, 2003. **22**(42): p. 6497-507.
54. Wu, G., X. Feng, and L. Stein, *A human functional protein interaction network and its application to cancer data analysis.* Genome Biol, 2010. **11**(5): p. R53.
55. Beenken, A. and M. Mohammadi, *The FGF family: biology, pathophysiology and therapy.* Nat Rev Drug Discov, 2009. **8**(3): p. 235-53.
56. Myoken, Y., et al., *Expression of fibroblast growth factor-1 (FGF-1), FGF-2 and FGF receptor-1 in a human salivary-gland adenocarcinoma cell line: evidence of growth.* Int J Cancer, 1996. **65**(5): p. 650-7.
57. Itoh, N. and D.M. Ornitz, *Fibroblast growth factors: from molecular evolution to roles in development, metabolism and disease.* J Biochem, 2011. **149**(2): p. 121-30.

58. Cotton, L.M., M.K. O'Bryan, and B.T. Hinton, *Cellular signaling by fibroblast growth factors (FGFs) and their receptors (FGFRs) in male reproduction.* Endocr Rev, 2008. **29**(2): p. 193-216.
59. Ornitz, D.M. and N. Itoh, *Fibroblast growth factors.* Genome Biol, 2001. **2**(3): p. REVIEWS3005.
60. Haddad, L.E., et al., *Characterization of FGF receptor expression in human neutrophils and their contribution to chemotaxis.* Am J Physiol Cell Physiol, 2011. **301**(5): p. C1036-45.
61. Beer, H.D., et al., *Fibroblast growth factor (FGF) receptor 1-IIIb is a naturally occurring functional receptor for FGFs that is preferentially expressed in the skin and the brain.* J Biol Chem, 2000. **275**(21): p. 16091-7.
62. Spinola, M., et al., *FGFR4 Gly388Arg polymorphism and prognosis of breast and colorectal cancer.* Oncol Rep, 2005. **14**(2): p. 415-9.
63. Wang, J., et al., *Altered fibroblast growth factor receptor 4 stability promotes prostate cancer progression.* Neoplasia, 2008. **10**(8): p. 847-56.
64. Wesche, J., K. Haglund, and E.M. Haugsten, *Fibroblast growth factors and their receptors in cancer.* Biochem J, 2011. **437**(2): p. 199-213.
65. van Rhijn, B.W., et al., *Novel fibroblast growth factor receptor 3 (FGFR3) mutations in bladder cancer previously identified in non-lethal skeletal disorders.* Eur J Hum Genet, 2002. **10**(12): p. 819-24.
66. Johnatty, S.E., et al., *Polymorphisms in the FGF2 gene and risk of serous ovarian cancer: results from the ovarian cancer association consortium.* Twin Res Hum Genet, 2009. **12**(3): p. 269-75.
67. Hendrix, N.D., et al., *Fibroblast growth factor 9 has oncogenic activity and is a downstream target of Wnt signaling in ovarian endometrioid adenocarcinomas.* Cancer Res, 2006. **66**(3): p. 1354-62.
68. Wei, W., et al., *FGF18 as a prognostic and therapeutic biomarker in ovarian cancer.* J Clin Invest, 2013. **123**(10): p. 4435-48.
69. Basu, M., et al., *FGF16 promotes invasive behavior of SKOV-3 ovarian cancer cells through activation of mitogen-activated protein kinase (MAPK) signaling pathway.* J Biol Chem, 2014. **289**(3): p. 1415-28.
70. Tebben, P.J., et al., *Elevated fibroblast growth factor 23 in women with malignant ovarian tumors.* Mayo Clin Proc, 2005. **80**(6): p. 745-51.
71. Coleman, A.B., et al., *Chemosensitization by fibroblast growth factor-2 is not dependent upon proliferation, S-phase accumulation, or p53 status.* Biochem Pharmacol, 2002. **64**(7): p. 1111-23.
72. Turkington, R.C., et al., *Fibroblast growth factor receptor 4 (FGFR4): a targetable regulator of drug resistance in colorectal cancer.* Cell Death Dis, 2014. **5**: p. e1046.
73. Coutu, D.L., M. Francois, and J. Galipeau, *Inhibition of cellular senescence by developmentally regulated FGF receptors in mesenchymal stem cells.* Blood, 2011. **117**(25): p. 6801-12.
74. Grose, R. and C. Dickson, *Fibroblast growth factor signaling in tumorigenesis.* Cytokine Growth Factor Rev, 2005. **16**(2): p. 179-86.

75. Chamorro, M.N., et al., *FGF-20 and DKK1 are transcriptional targets of beta-catenin and FGF-20 is implicated in cancer and development.* EMBO J, 2005. **24**(1): p. 73-84.
76. Cole, C., et al., *Inhibition of FGFR2 and FGFR1 increases cisplatin sensitivity in ovarian cancer.* Cancer Biol Ther, 2010. **10**(5): p. 495-504.
77. Ficz, G., et al., *FGF signaling inhibition in ESCs drives rapid genome-wide demethylation to the epigenetic ground state of pluripotency.* Cell Stem Cell, 2013. **13**(3): p. 351-9.
78. Crickard, K., et al., *Basic fibroblast growth factor and receptor expression in human ovarian cancer.* Gynecol Oncol, 1994. **55**(2): p. 277-84.
79. Obermair, A., et al., *Influence of intratumoral basic fibroblast growth factor concentration on survival in ovarian cancer patients.* Cancer Lett, 1998. **130**(1-2): p. 69-76.
80. Birrer, M.J., et al., *Whole genome oligonucleotide-based array comparative genomic hybridization analysis identified fibroblast growth factor 1 as a prognostic marker for advanced-stage serous ovarian adenocarcinomas.* J Clin Oncol, 2007. **25**(16): p. 2281-7.
81. Whitworth, M.K., et al., *Regulation of fibroblast growth factor-2 activity by human ovarian cancer tumor endothelium.* Clin Cancer Res, 2005. **11**(12): p. 4282-8.
82. Tsang, T.Y., Mohapatra, G., Itamochi, H., Mok, S.C., and Birrer, M.J. *Identification of FGFR3 as a potential therapeutic target gene for human clear cell ovarian cancer by global genomic analysis. Abstract 1528*. in *105th Annual Meeting of the American Association for Cancer Research, 2014 Apr 5-9;* . 2014. SAn Diego, CA: American Association of Cancer Research.
83. Gan, Y., M.G. Wientjes, and J.L. Au, *Expression of basic fibroblast growth factor correlates with resistance to paclitaxel in human patient tumors.* Pharm Res, 2006. **23**(6): p. 1324-31.
84. Smith, G., et al., *Individuality in FGF1 expression significantly influences platinum resistance and progression-free survival in ovarian cancer.* Br J Cancer, 2012. **107**(8): p. 1327-1336.
85. Song, S., et al., *Fibroblast growth factors: an epigenetic mechanism of broad spectrum resistance to anticancer drugs.* Proc Natl Acad Sci U S A, 2000. **97**(15): p. 8658-63.
86. Davidson, B.A., et al., *Differential Angiogenic Gene Expression in TP53 Wild-Type and Mutant Ovarian Cancer Cell Lines.* Front Oncol, 2014. **4**: p. 163.
87. Ab Mutalib, N.S., et al., *Molecular characterization of serous ovarian carcinoma using a multigene next generation sequencing cancer panel approach.* BMC Res Notes, 2014. **7**: p. 805.
88. Johnatty, S.E., et al., *Polymorphisms in the FGF2 gene and risk of serous ovarian cancer: results from the ovarian cancer association consortium.* Twin Res Hum Genet, 2009. **12**(3): p. 269-75.
89. Jeffers, M., et al., *Identification of a novel human fibroblast growth factor and characterization of its role in oncogenesis.* Cancer Res, 2001. **61**(7): p. 3131-8.

90. Ohmachi, S., et al., *Preferential neurotrophic activity of fibroblast growth factor-20 for dopaminergic neurons through fibroblast growth factor receptor-1c.* J Neurosci Res, 2003. **72**(4): p. 436-43.
91. Zhang, X., et al., *Receptor specificity of the fibroblast growth factor family. The complete mammalian FGF family.* J Biol Chem, 2006. **281**(23): p. 15694-700.
92. Chell, V., et al., *Tumour cell responses to new fibroblast growth factor receptor tyrosine kinase inhibitors and identification of a gatekeeper mutation in FGFR3 as a mechanism of acquired resistance.* Oncogene, 2013. **32**(25): p. 3059-70.

Appendix 1

Figure 1

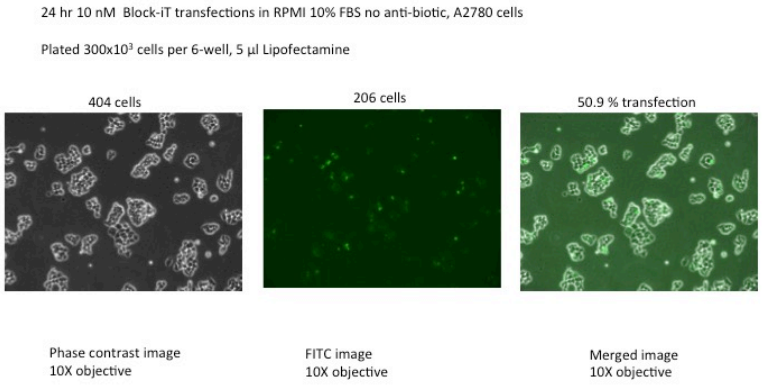

Figure 2

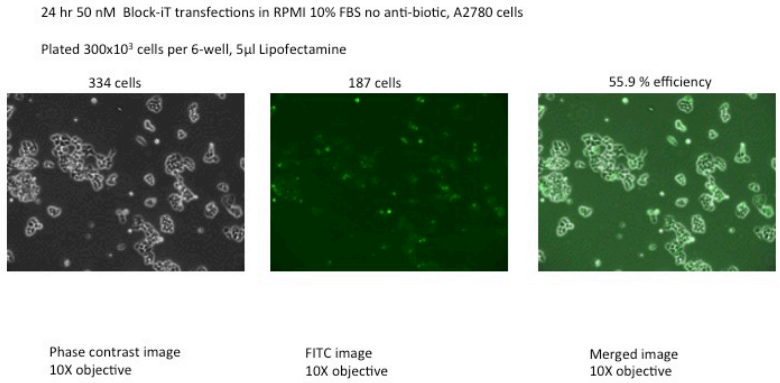

Figure 3

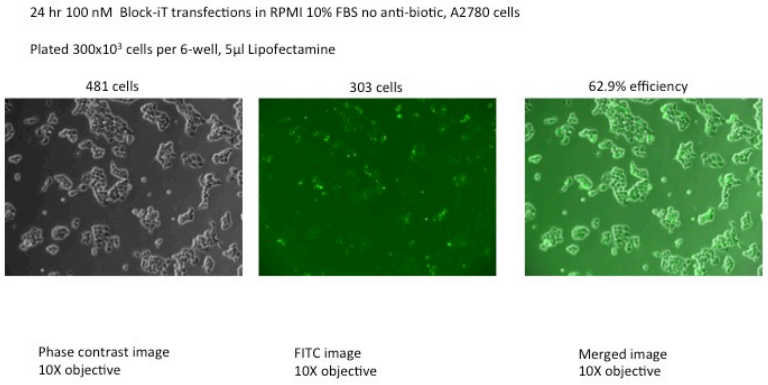

Figure 4

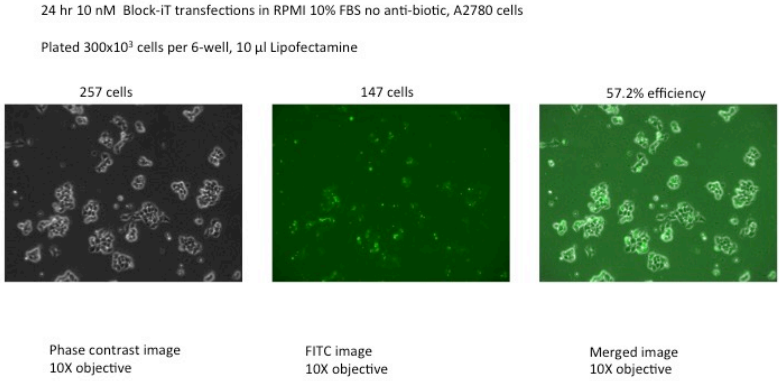

Figure 5

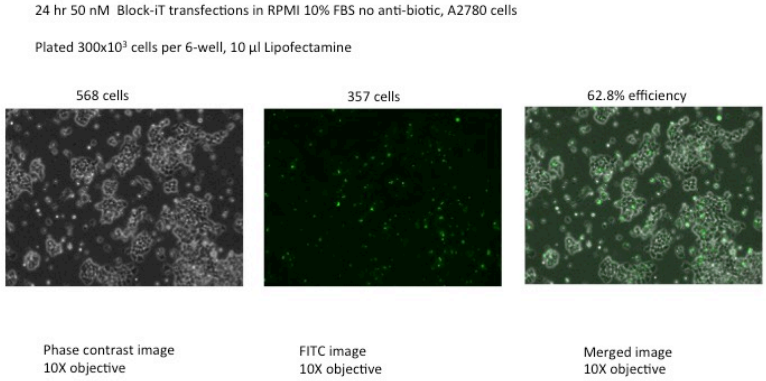

Figure 6

Figure 7

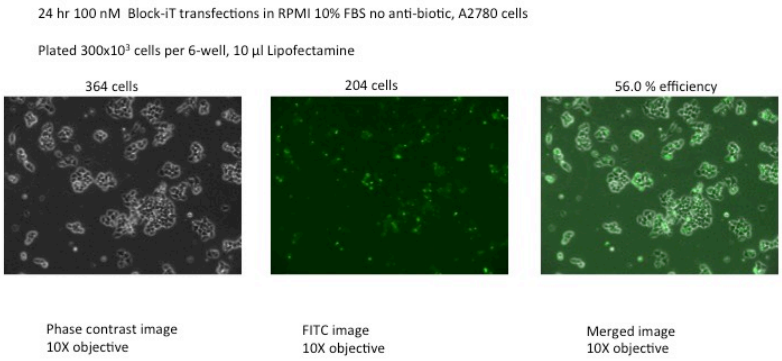

Appendix 2

Figure 1

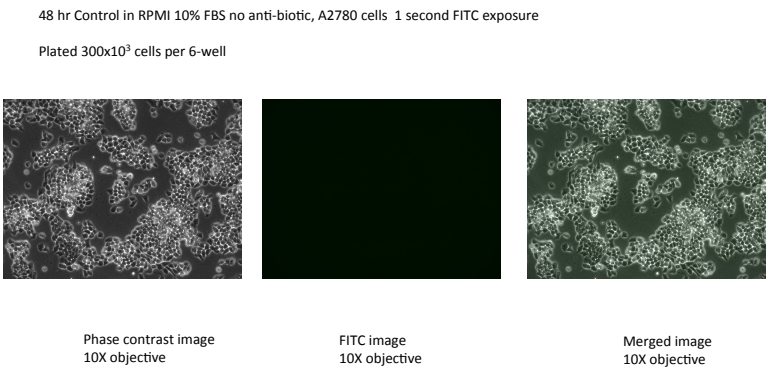

Figure 2

48 hr Control in RPMI 10% FBS no anti-biotic, A2780 cells, 5 second FITC exposure

Plated 300x10^3 cells per 6-well

Phase contrast image
10X objective

FITC image
10X objective

Merged image
10X objective

Figure 3

Figure 4

48 hr 10 nM Block-iT transfections in RPMI 10% FBS no anti-biotic, A2780 cells

Plated 300x10^3 cells per 6-well, 5µl Lipofectamine

626 cells

190 cells

30.3 % efficiency

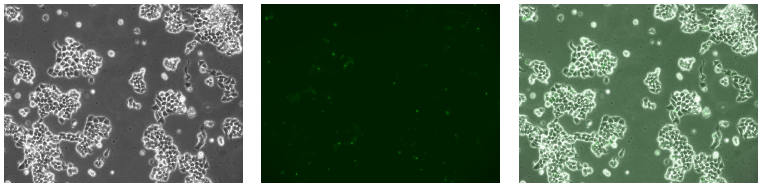

Phase contrast image
10X objective

FITC image
10X objective

Merged image
10X objective

Figure 5

48 hr 10 nM Block-iT transfections in OPTIMEM no anti-biotic, A2780 cells

Plated 300x10^3 cells per 6-well, 5µl Lipofectamine

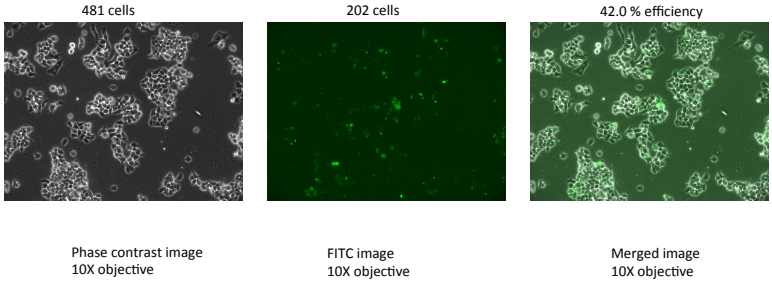

Figure 6

48 hr 50 nM Block-iT transfections in RPMI 10% FBS no anti-biotic, A2780 cells

Plated 300x10^3 cells per 6-well, 5µl Lipofectamine

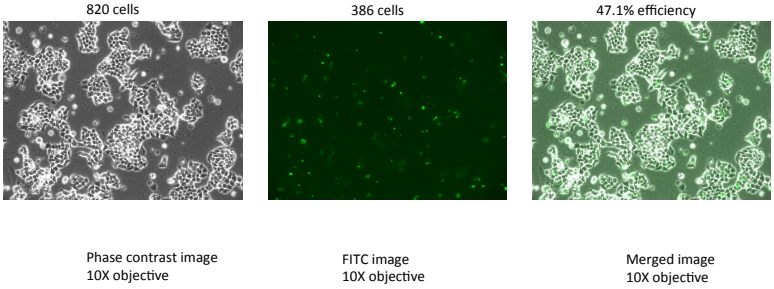

Figure 7

48 hr 50 nM Block-iT transfections in OPTIMEM no anti-biotic, A2780 cells

Plated 300x10^3 cells per 6-well, 5µl Lipofectamine

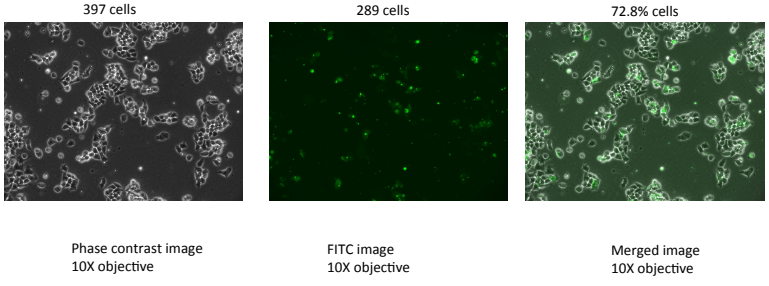

Figure 8

48 hr 100 nM Block-iT transfections in RPMI 10% FBS no anti-biotic, A2780 cells

Plated 300x10^3 cells per 6-well, 5µl Lipofectamine

689 cells

530 cells

76.9 % efficiency

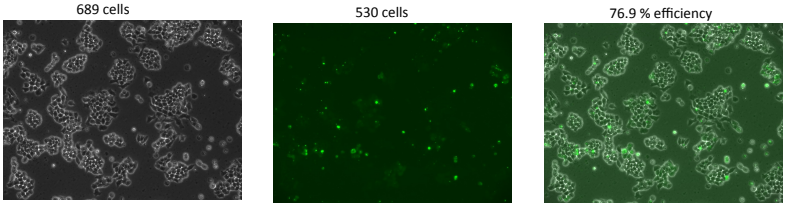

Phase contrast image
10X objective

FITC image
10X objective

Merged image
10X objective

Figure 9

48 hr 100 nM Block-iT transfections in OPTIMEM no anti-biotic, A2780 cells

Plated 300x10^3 cells per 6-well, 5µl Lipofectamine

582 cells

414 cells

71.1% efficiency

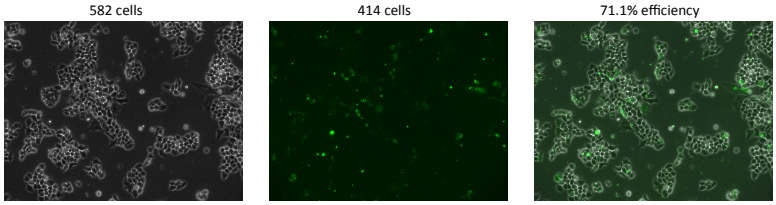

Phase contrast image
10X objective

FITC image
10X objective

Merged image
10X objective

Figure 10

48 hr 10 nM Block-iT transfections in RPMI 10% FBS no anti-biotic, A2780 cells

Plated 300x10^3 cells per 6-well, 10 µl Lipofectamine

413 cells

294 cells

71.1 % efficiency

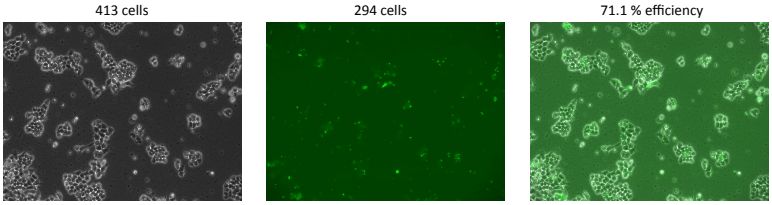

Phase contrast image
10X objective

FITC image
10X objective

Merged image
10X objective

Figure 11

48 hr 10 nM Block-iT transfections in OPTIMEM no anti-biotic, A2780 cells

Plated 300x10^3 cells per 6-well, 10 µl Lipofectamine

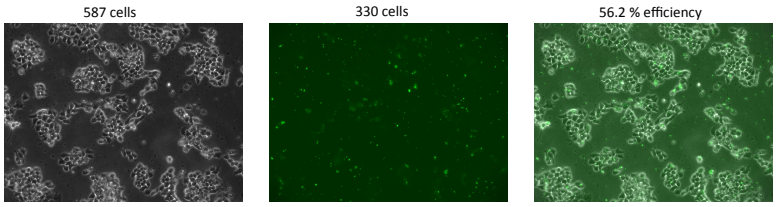

Figure 12

48 hr 50 nM Block-iT transfections in RPMI 10% FBS no anti-biotic, A2780 cells

Plated 300x10^3 cells per 6-well, 10 µl Lipofectamine

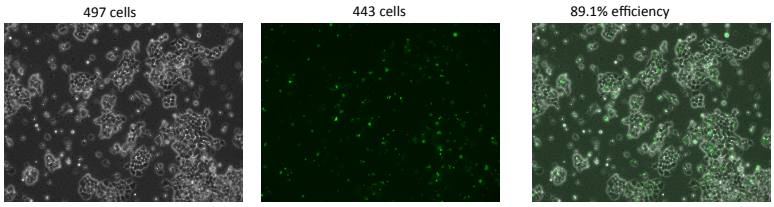

Figure 13

48 hr 50 nM Block-iT transfections in OPTIMEM no anti-biotic, A2780 cells

Plated 300x10^3 cells per 6-well, 10 µl Lipofectamine

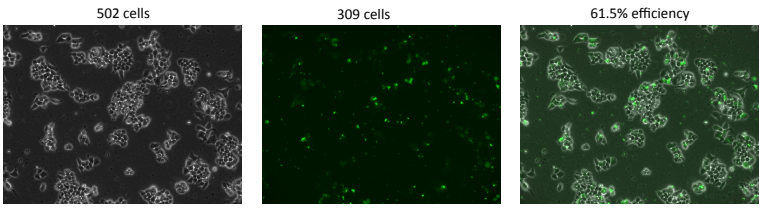

Figure 14

48 hr 100 nM Block-iT transfections in RPMI 10% FBS no anti-biotic, A2780 cells

Plated 300x10^3 cells per 6-well, 10 µl Lipofectamine

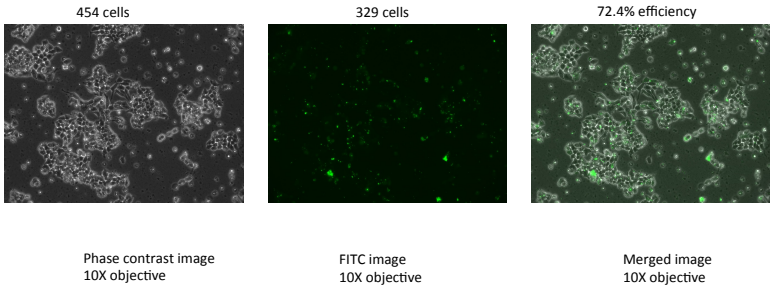

Figure 16

48 hr 100 nM Block-iT transfections in OPTIMEM no anti-biotic, A2780 cells

Plated 300x10^3 cells per 6-well, 10 µl Lipofectamine

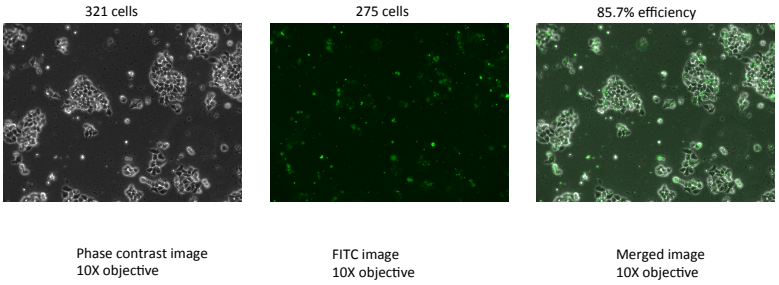

Appendix 3

Figure 1

72 hr Control in RPMI 10% FBS no anti-biotic, A2780 cells 1 second FITC exposure

Plated 300x10^3 cells per 6-well

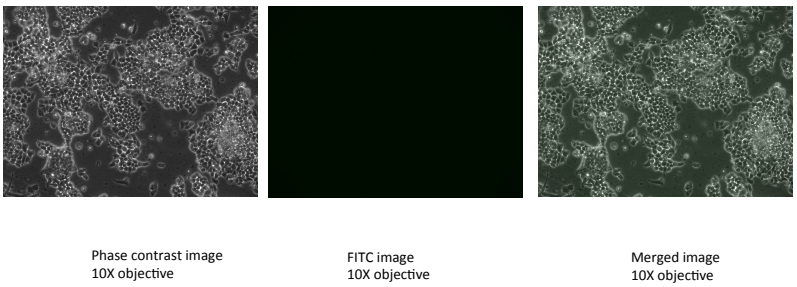

Figure 2

72 hr Control in RPMI 10% FBS no anti-biotic, A2780 cells, 5 second FITC exposure

Plated 300x10^3 cells per 6-well

Phase contrast image
10X objective

FITC image
10X objective

Merged image
10X objective

Figure 3

72 hr 10 nM Block-iT transfections in RPMI 10% FBS no anti-biotic, A2780 cells

Plated 300x10^3 cells per 6-well, 5µl Lipofectamine

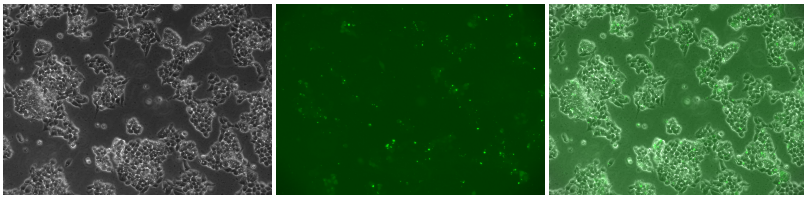

Phase contrast image
10X objective

FITC image
10X objective

Merged image
10X objective

Figure 4

72 hr 50 nM Block-iT transfections in RPMI 10% FBS no anti-biotic, A2780 cells

Plated 300x10^3 cells per 6-well, 5µl Lipofectamine

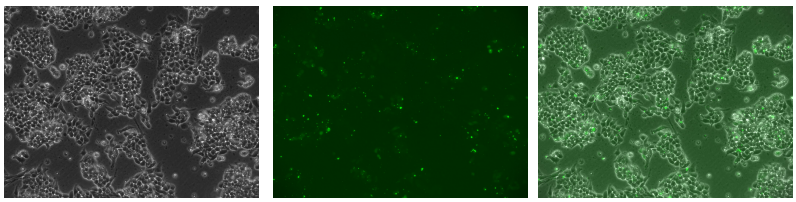

Phase contrast image
10X objective

FITC image
10X objective

Merged image
10X objective

Figure 5

72 hr 100 nM Block-iT transfections in RPMI 10% FBS no anti-biotic, A2780 cells

Plated 300x10^3 cells per 6-well, 5µl Lipofectamine

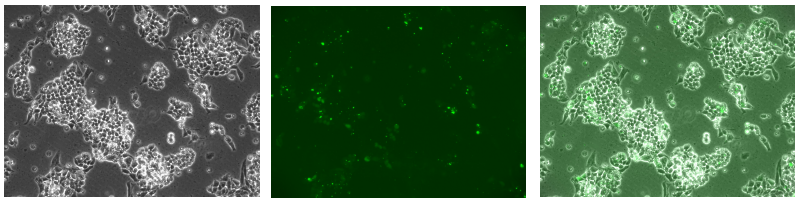

Phase contrast image
10X objective

FITC image
10X objective

Merged image
10X objective

Figure 6

72 hr 10 nM Block-iT transfections in RPMI 10% FBS no anti-biotic, A2780 cells

Plated 300x10^3 cells per 6-well, 10 µl Lipofectamine

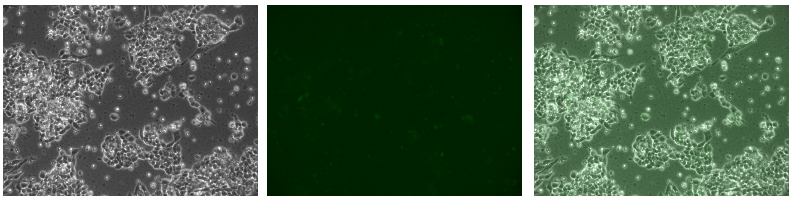

Phase contrast image
10X objective

FITC image
10X objective

Merged image
10X objective

Figure 7

72 hr 50 nM Block-iT transfections in RPMI 10% FBS no anti-biotic, A2780 cells

Plated 300x10^3 cells per 6-well, 10 µl Lipofectamine

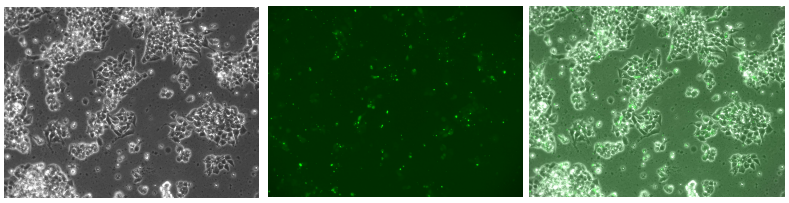

Phase contrast image
10X objective

FITC image
10X objective

Merged image
10X objective

Figure 8

72 hr 100 nM Block-iT transfections in RPMI 10% FBS no anti-biotic, A2780 cells

Plated 300x10^3 cells per 6-well, 10 µl Lipofectamine

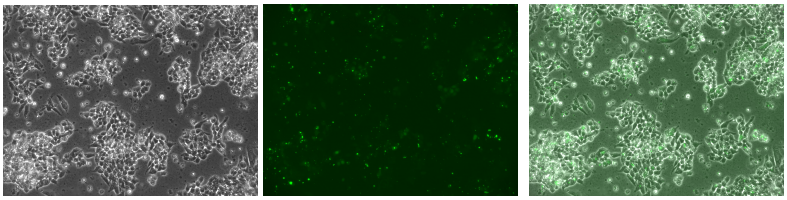

Phase contrast image
10X objective

FITC image
10X objective

Merged image
10X objective